






Plasmid-encoded toxin defence mediates mutualistic microbial interactions

Received: 18 July 2022

Accepted: 11 October 2023

Published online: 27 December 2023

 Check for updates

Sarah Morais ^{1,2,3}, Michael Mazor^{1,2,3}, Omar Tovar-Herrera^{1,2,3}, Tamar Zehavi^{1,2,3}, Alvah Zorea ^{1,2,3}, Morya Ifrach¹, David Bogumil^{1,2,3}, Alexander Brandis⁴, Jens Walter ⁵, Natalie Elia^{1,2}, Eyal Gur^{1,2} & Itzhak Mizrahi ^{1,2,3} 

Gut environments harbour dense microbial ecosystems in which plasmids are widely distributed. Plasmids facilitate the exchange of genetic material among microorganisms while enabling the transfer of a diverse array of accessory functions. However, their precise impact on microbial community composition and function remains largely unexplored. Here we identify a prevalent bacterial toxin and a plasmid-encoded resistance mechanism that mediates the interaction between Lactobacilli and Enterococci. This plasmid is widespread across ecosystems, including the rumen and human gut microbiota. Biochemical characterization of the plasmid revealed a defence mechanism against reuterin, a toxin produced by various gut microbes, such as *Limosilactobacillus reuteri*. Using a targeted metabolomic approach, we find reuterin to be prevalent across rumen ecosystems with impacts on microbial community structure. *Enterococcus* strains carrying the protective plasmid were isolated and their interactions with *L. reuteri*, the toxin producer, were studied in vitro. Interestingly, we found that by conferring resistance against reuterin, the plasmid mediates metabolic exchange between the defending and the attacking microbial species, resulting in a beneficial relationship or mutualism. Hence, we reveal here an ecological role for a plasmid-coded defence system in mediating a beneficial interaction.

Plasmids are circular self-replicating double-stranded DNA molecules that reside within bacterial hosts¹. Plasmids have been recognized as key vectors of genetic exchange between microbial chromosomes. Their high abundance in microbial populations sampled from various habitats indicates that they have an important ecological role². Despite their apparent great importance in nature, the role of plasmids within microbial communities is poorly understood, as they are usually studied as individual entities within specific hosts, neglecting the environmental and community context.

Plasmids are composed of a conserved DNA backbone that includes replication and mobilization genes, which are important for plasmid maintenance within their specific host and transfer among

other microbial hosts. They also carry a variable assortment of accessory genes, which often contribute to the phenotypic diversity of their host. Plasmids isolated from different environments encode a versatile array of accessory functions, ranging from antibiotic resistance to nitrogen fixation^{3,4}. These plasmid-borne functions may confer an advantage upon their host in its local environment, making the burden of carrying the plasmid worthwhile to the host organism^{2,5-9}.

Knowledge of the biology of plasmids and the functions that are mobilized by them can provide insights into the genetic interactions and the ecological roles played by plasmids in individual microbial species and complex microbial communities. Although generally studied in individual species, the role of plasmids can be even greater

¹National Institute of Biotechnology in the Negev, Ben-Gurion University of the Negev, Be'er Sheva, Israel. ²Department of Life Sciences, Ben-Gurion University of the Negev, Be'er Sheva, Israel. ³The Goldman Sonnenfeldt School of Sustainability and Climate Change, Ben-Gurion University of the Negev, Be'er Sheva, Israel. ⁴Life Sciences Core Facilities, Weizmann Institute of Science, Rehovot, Israel. ⁵Department of Medicine, University College Cork, Cork, Ireland. ✉e-mail: imizrahi@bgu.ac.il

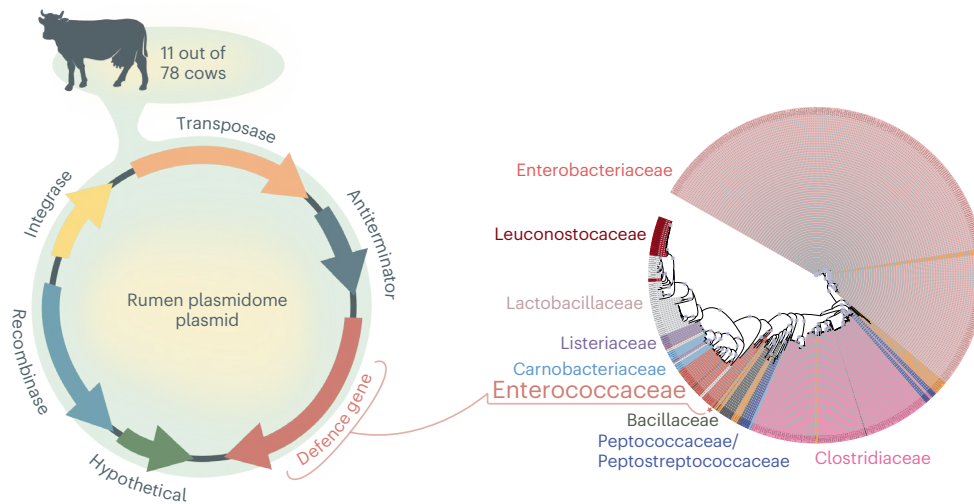


Fig. 1 | Identification of rumen plasmid with potential ecological relevance from the rumen plasmidome. Left: plasmid map of 1,3-PD plasmid retrieved from the rumen microbiome of a 78-animal cohort. Right: phylogenetic tree of 1,3-PD genes retrieved by PhyloGenie²¹ from the NR NCBI database. Bacillaceae, Clostridiaceae, Enterobacteriaceae, Enterococcaceae, Lactobacillaceae, Leuconostocaceae and Listeriaceae families are colour coded and appear on the tree. Proteins

assigned to Carnobacteriaceae family are labelled in light blue, Peptococcaceae/Peptostreptococcaceae in darker blue and other phylogenies in light orange (including the Planococcaceae, Pseudomonadaceae, Thermoactinomycetaceae, Yersiniaceae, Fusobacteriaceae, Moraxellaceae and Morganeliaceae families). A red star and a red square mark the position of the 1,3-PD rumen plasmidome gene. Bootstrapping higher than 0.9 is indicated by a blue circle.

in dense microbial communities where close proximity exists among microbial individuals of different lineages¹⁰. In such dense communities, the ecological role of plasmids as accessory gene carriers can be instrumental to niche expansion, as they allow acquisition of potential functions relevant to resource utilization, as well as weapons and defence mechanisms, thereby expanding the niche space^{10,11}.

The rumen microbial ecosystem is one of the most studied complex microbial environments due to its importance to agriculture, potential for comprehending fibre-degradation principles, contribution to carbon cycling and bioenergy, and its link to environmental issues, notably the greenhouse effect^{12,13}. This complex microbial community is composed of a multitude of different microbial species co-residing at a density greater than 10^{11} ml⁻¹, thus rendering this ecosystem ideal for studying the role of plasmids in microbial community ecology. We focused on this system to gain further insights into the ecological role of plasmids in their natural environments. To this end, we identified prevalent natural plasmid candidates with the underlying assumption that plasmids with high occupancy encoding for metabolic accessory genes could provide insights to elucidate plasmid-mediated ecology.

In our previous explorations of the plasmidome^{14,15}, we have reported that the mobile genetic pool carries highly diverse accessory genes with potentially high ecological relevance. In the current study, we explored accessory rumen plasmidome genes for recurring functions with high occupancy across multiple ecosystems and their importance within them. Our findings reveal the widespread occurrence of a plasmid accessory function in the rumen and human gut systems that provides resistance to a toxin and facilitates a mutualistic relationship between toxin-producing and plasmid-carrying defending microbes, suggesting a pivotal role for plasmids in orchestrating higher-order microbial interactions.

Results

Enterococcal plasmid-borne 1,3-propanediol dehydrogenase (1,3-PD) is widespread in the rumen

We have previously identified many unconventional accessory functions that are carried on plasmids within the environment^{14,15}. Here we aimed to explore the potential ecological role of a plasmid encoding one such putative function, the 1,3-PD gene that we found

to be carried in high abundance within the rumen plasmidome^{14,15}. This putative function was found to be coded on plasmids coming from 11 samples out of 78 metagenomes from our previous study¹⁶. These metagenome-assembled rumen plasmids were assembled via Recycler algorithm¹⁷ and extracted from metagenomic reads or sequencing of extracted plasmidomes, as described in previous studies^{15,18,19}. This finding raised the hypothesis that this putative gene could have high ecological relevance, as it occurs repeatedly in the mobile genetic pool. In all cases, the putative (1,3-PD) gene was identified in a 5,326-bp plasmid that did not contain any mobilization genes coding for plasmid transmissibility (Supplementary Table 1). This suggests that the plasmid is constrained to its bacterial hosts or transferred by a non-conjugative mechanism²⁰. The plasmid contains additional putative genes, annotated as recombinase, integrase, transposase and antiterminator functions.

We next applied a gene-tree approach to determine the phylogeny of the plasmidic 1,3-PD gene by retrieving homologue genes from the NR NCBI database and phylogenetically classifying the 1,3-PD genes using the PhyloGenie pipeline²¹. This analysis positioned the plasmid coding the 1,3-PD gene within the Enterococcaceae family clade and suggested that its members represented the host microbes of these plasmids (Fig. 1).

1,3-PD plasmid is suspected to protect against reuterin toxin

The 1,3-PD enzymes were reported to be part of a chromosomal operon coding for glycerol fermentation to propionate²². The fact that only the 1,3-PD putative gene was coded on the rumen plasmid suggested that it might pose a different ecological role from that of glycerol fermentation. Studies have shown that genes carried on plasmids can be expressed at higher levels compared with their chromosomal counterparts. This higher expression could confer a selective advantage to bacteria carrying the plasmid with the defence gene, allowing them to better compete with other bacterial species for resources in their environment²³. A literature search revealed that the 3-hydroxypropionaldehyde molecule, also referred to as reuterin, has antimicrobial activity and is often produced by gut microbes, notably *Limosilactobacillus reuteri* (Fig. 2a inset)^{24,25}. Thus, we considered the possibility that the putative rumen plasmid gene might function as a defence mechanism against the antibacterial activity of

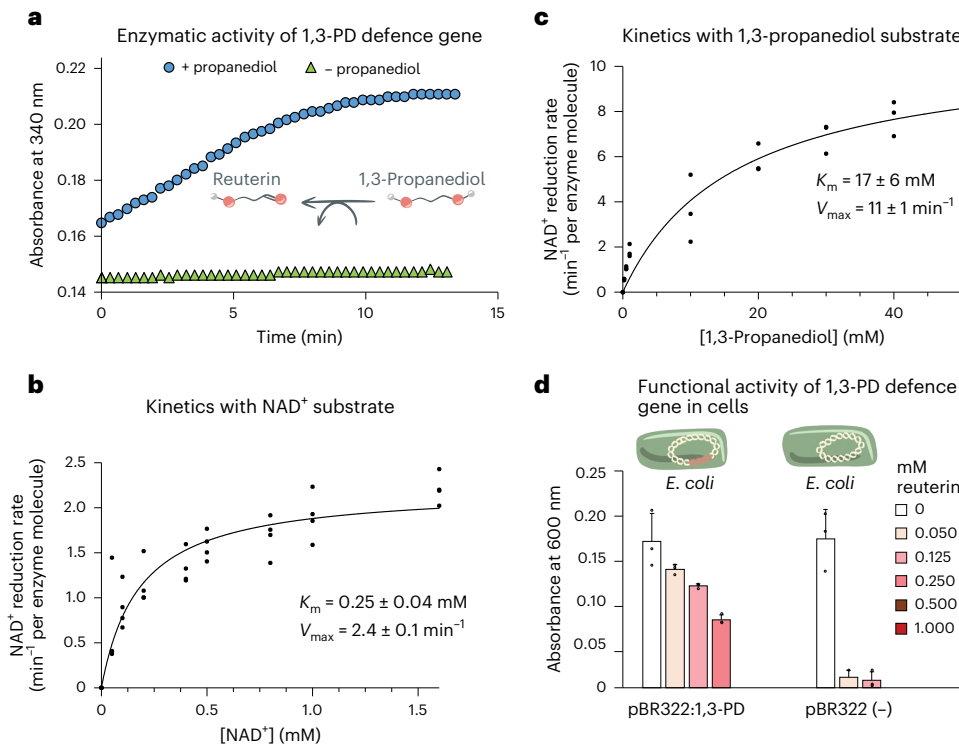


Fig. 2 | Biochemical characterization of the 1,3-PD defence gene and its functional activity within a bacterial host. **a**, Enzymatic activity of the 1,3-PD enzyme over time, using 1,3-propanediol as a substrate. **b, c**, Michaelis–Menten analysis of 1,3-PD activity at increasing concentrations of either NAD⁺ (**b**) or 1,3-propanediol (**c**). The measurements were carried out in technical triplicates, for which actual data are presented. The solid curves were generated by fitting the Michaelis–Menten equation to the data, assuming non-cooperative binding of NAD⁺ and 1,3-propanediol by the enzyme. **d**, Protective effect against reuterin

of 1,3-PD expression in *E. coli*. ER2566 strains constitutively expressing 1,3-PD from plasmid pBR322 were grown in increasing concentrations of reuterin (0 to 1 mM final concentration) in 200 μ l of LB medium (volumes of cultures were homogenized across samples using sterile water). Following 24 h at 37 °C, turbidity was measured at 600 nm. Control strains carried an empty vector. The measurements were carried out in biological triplicates, for which actual data, averages and standard deviations are presented.

reuterin. A basic local alignment search tool (Blast) against the NR database of the putative rumen plasmid 1,3-PD gene variant revealed 74% amino-acid sequence identity and 82% similarity to the previously characterized 1,3-PD from *Clostridium butyricum*²² and showed high similarities with other previously characterized enzymes from this family (Extended Data Fig. 1)^{22,26–28}. This further suggested that this putative plasmid-coded enzyme converts reuterin into 1,3-propanediol and therefore detoxifies it.

1,3-PD gene is active in vitro and detoxifies antibacterial reuterin

We tested whether 1,3-PD can detoxify reuterin, by cloning the gene and overexpressing the enzyme in *E. coli*. The purified enzyme was clearly found to be active via measurement of oxidation by NAD⁺ of, rather than reuterin, the commercially available 1,3-propanediol, by monitoring the absorbance of the formed NADH at 340 nm (Fig. 2a). Next, we sought to assess the enzyme's affinity to its substrates. Accordingly, titration experiments were carried out, where NAD⁺ reduction rates were measured at increasing concentrations of NAD⁺ or 1,3-propanediol. The results yielded classic Michaelis–Menten curves, with a K_m of 0.25 ± 0.04 mM for NAD⁺ (Fig. 2b and Extended Data Fig. 2) and a K_m of 17 ± 6 mM (Fig. 2c and Extended Data Fig. 2) for 1,3-propanediol. As 1,3-propanediol titrations were carried out with NAD⁺ concentrations that were close to saturation, the resulting V_{max} value (11 ± 1 min⁻¹ per enzyme molecule) extracted from the resulting data (Fig. 2c) closely corresponded to the enzyme catalytic rate constant (k_{cat}). These kinetic parameters closely resemble the values previously reported for the homologous enzyme from *Klebsiella pneumoniae*^{27,29}, suggesting that reuterin inactivation might be the role of the plasmid-coded enzyme in the rumen.

Plasmid-encoded 1,3-PD protects bacterial cells from reuterin toxin

As the plasmid-coded 1,3-PD defence gene was not part of a full operon but a standalone gene on the plasmid, we next tested whether it would confer reuterin resistance in bacterial cells. To this end, we cloned the gene into an *E. coli* plasmid pBR322 under the beta-lactamase promoter and, following transformation, grew the bacteria at increasing concentrations of reuterin (0 to 1 mM final concentration) compared to the control. The results of this experiment showed that in all reuterin concentrations, the strain carrying the 1,3-PD defence gene exhibited significantly higher survival rates than the control strain lacking the gene, the latter showing no apparent growth above 0.125 mM reuterin, thus demonstrating the protective effect of the 1,3-PD defence enzyme against reuterin (Fig. 2d). The protective effect of the enzyme decreased at higher reuterin concentrations of 0.5 and 1 mM where no growth of both strains was observed, with a half maximal inhibitory concentration (IC_{50}) value between 0.125 mM and 0.25 mM reuterin.

Reuterin is prevalent across and influences rumen ecosystems

As our findings show that reuterin has an effect on bacterial cells and the plasmid carrying the 1,3-PD defence gene could confer reuterin resistance in bacterial cells, we first examined whether reuterin is present in natural rumen ecosystems. To this end, we measured reuterin concentrations in 20 bovine rumen samples using an LC–MS-targeted metabolomics approach. Our findings showed that reuterin is indeed present in 10 of the 20 rumen samples in concentrations ranging from 0.07 to 0.89 mM (Fig. 3a).

To examine the effect of reuterin and the defence system on members of the rumen ecosystem, we exposed to reuterin selected

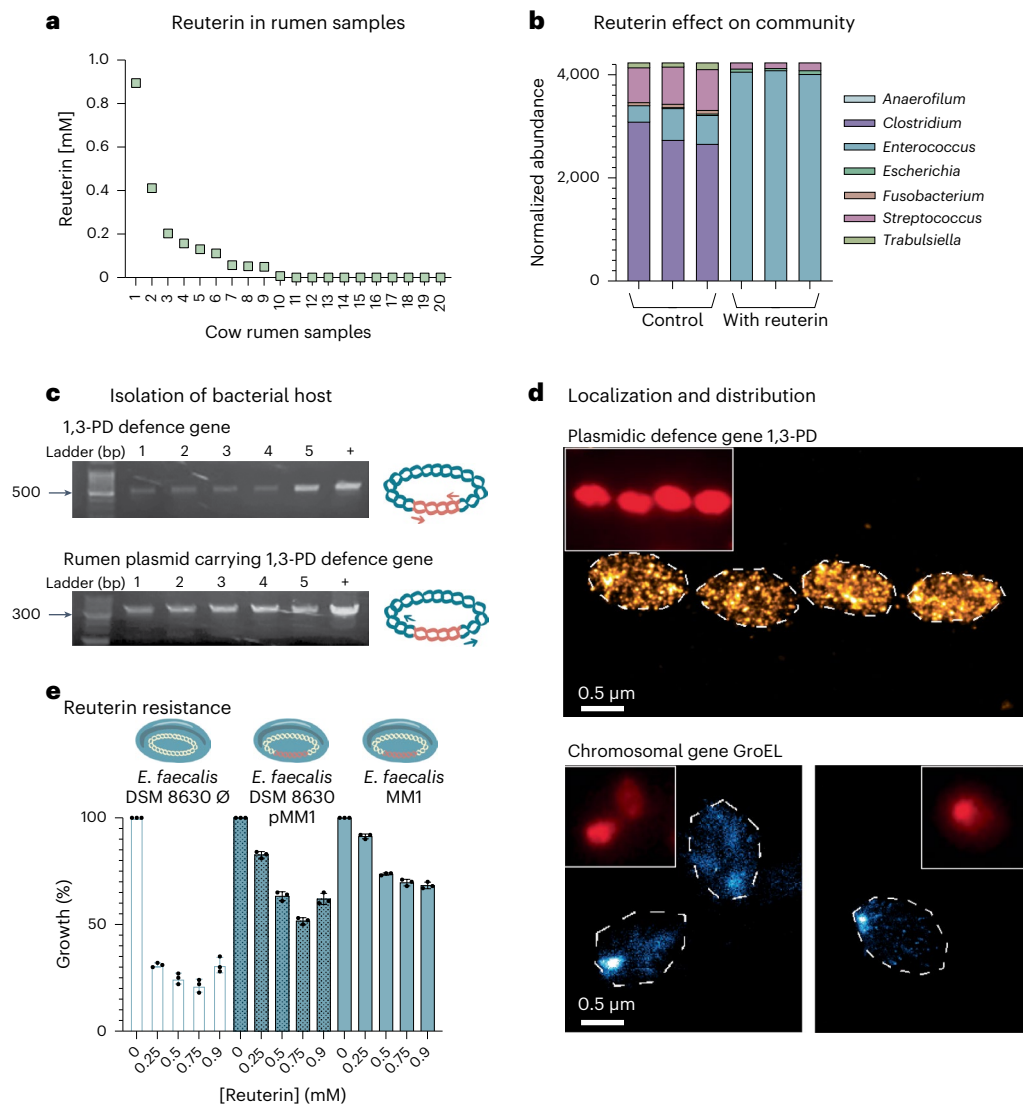


Fig. 3 | Effect of reuterin on rumen microbial composition and isolation of the bacterial host. **a**, Distribution plot representing the concentration of reuterin (in mM) detected in rumen samples from 20 cows. **b**, Phylogenetic analysis of the cultured microbial rumen community after serial passaging with or without reuterin addition at the genus level. The bar graph represents the normalized abundances of the genera. Genera with low abundances in control communities, including *Adlercreutzia*, *Bacteroides*, *Bifidobacterium*, *Blautia*, *Butyrivibrio*, *Butyrivibrio*, *Dialister*, *Peptococcus*, *Prevotella*, *Roseburia* and *Sediminibacterium*, are not represented. **c**, Top gel: PCR of part of the 1,3-PD gene (expected product length 560 bp), amplified from the plasmid-purified fraction of five isolates. Bottom gel: PCR of the whole plasmid encoding the 1,3-PD gene, using reverse primers (expected product length ~5,300 bp), amplified from the plasmid-purified fraction of five isolates. In both gels, plasmid pBR322:1,3-PD was used as a positive control template. Both gels were reproducible in two distinct experiments. Illustrations on the right represent the plasmid in blue, and the 1,3-PD gene in orange and arrows indicate the primers used for the PCR.

d, STORM and wide-field (inset) imaging of *E. faecalis* MM1 cells labelled by CARD-FISH with specific probes for the 1,3-PD defence plasmidic gene (top) or GroEL chromosomal gene (bottom). White dashed lines delimit the bacterial cell walls. Similar images were obtained from two distinct experiments.

e, Comparative resistance of *E. faecalis* MM1 plasmid-carrying strain and *E. faecalis* DSM 8630 pMM1 transformed with the rumen plasmid with the 1,3-PD defence gene against reuterin and *E. faecalis* DSM 8630 Ø (with an empty plasmid backbone lacking the 1,3-PD defence gene). The strains were grown at increasing concentrations of reuterin (0 to 0.9 mM) in 1,000 µl basal defined medium and incubated for 24 h at 37 °C (volumes of cultures were homogenized across samples using sterile water). Turbidity measurements at 600 nm were used to determine the protection of the 1,3-PD defence gene against reuterin. The y axis represents the % growth of a specific strain as compared to growth of the same strain without reuterin. The measurements were carried out in biological triplicates, for which actual data, averages and standard deviations are presented.

rumen microcosms in which the plasmid was bioinformatically detected. A taxonomic analysis of the 16S ribosomal (r)RNA gene showed a significant increase in the relative abundance of the *Enterococcus* genus (from 7% to 96%) in the reuterin-treated microcosms compared with the more diverse community phenotypes without the addition of reuterin (Fig. 3b); results are in accordance with our bioinformatic analysis for the phylogenetic assignment of the Enterococcaceae family members as microbial hosts of the rumen plasmid containing 1,3-PD defence gene. The broad growth inhibition

of reuterin affected many rumen bacteria observed here, aligning with an earlier study demonstrating that reuterin altered the growth of the majority of the tested intestinal bacteria³⁰. Moreover, the increase in *Enterococcus* abundance was accompanied by an overall increase in biomass, as measured by total 16S rRNA copy number using qPCR (Extended Data Fig. 3; *t*-test *P* = 0.028). These findings suggest that the reduced competition among a less diverse bacterial community allowed for the proliferation of Enterococci in the reuterin-treated microcosms.

1,3-PD plasmid in *E. faecalis* isolates confers reuterin resistance

Following our above-described results that revealed an enrichment of the Enterococcaceae family in reuterin-treated rumen samples, we tested whether we could use reuterin to enrich and isolate microbes that carry the plasmid with the 1,3-PD defence gene. The reuterin-resistant enriched microbial community was used for selection on reuterin-containing agar plates. Plates containing high concentrations of reuterin presented an increased number of a specific type of colony morphology. Taxonomic identification of these colonies by 16S rRNA gene Sanger sequencing showed 95% identity to members of the Enterococcaceae family, specifically to *E. faecalis* strains, as predicted by our bioinformatics analysis. We therefore designated the new isolated strain as *E. faecalis* MM1. We also validated the presence of the plasmid carrying the 1,3-PD defence gene in these isolates by applying PCR (Fig. 3c) and a microscopic approach using a catalysed reporter deposition single-molecule fluorescence in situ hybridization (CARD-FISH) probe that targets the 1,3-PD defence gene, which was then visualized by stochastic optical reconstruction microscopy (STORM) (Fig. 3d). Using both approaches, we observed an exclusive and unique signal only for the isolated *E. faecalis* MM1 cells, but not for *E. faecalis* DSM 8630 strain lacking the plasmid (Fig. 3c,d and Extended Data Fig. 4). With the microscopic approach, we observed a scattered localization of signal when the cells were stained with the 1,3-PD-specific probe, as opposed to the confined localization observed using a different probe that targets the GroEL gene that is localized on the chromosome. We then performed whole-genome sequencing of one of the isolated strains together with a DSM strain of *E. faecalis*. We found that the two strains have an average nucleotide identity of 98.87% (ref. 31), with an extensive overlap of contigs (Extended Data Fig. 5). We then measured the reuterin resistance of the *E. faecalis* MM1 plasmid-carrying strain against that of *E. faecalis* DSM 8630 to which the pMM1 plasmid was transformed (*E. faecalis* DSM 8630 pMM1) and *E. faecalis* DSM 8630 \emptyset to which an empty plasmid backbone was transformed (Fig. 3e). Our results show that the *E. faecalis* MM1 culture and *E. faecalis* DSM 8630 pMM1 exhibited similar higher resistance patterns across the elevated concentrations of reuterin in the medium, as compared with *E. faecalis* DSM 8630 \emptyset , further supporting the importance of the plasmid in the defence against reuterin.

Mutualism and metabolic exchange between the two rival species

The high occurrence of the plasmid carrying the 1,3-PD defence gene in the rumen ecosystem and within the *E. faecalis* strain raised the question of whether the bacterial hosts carrying the 1,3-PD defence plasmid benefit from additional advantages other than reuterin resistance. Inspired by the symbiotic relationships that exist in nature³², we speculated that a potential benefit for carrying the defence plasmid would be a dependence on close proximity since reuterin is most effective

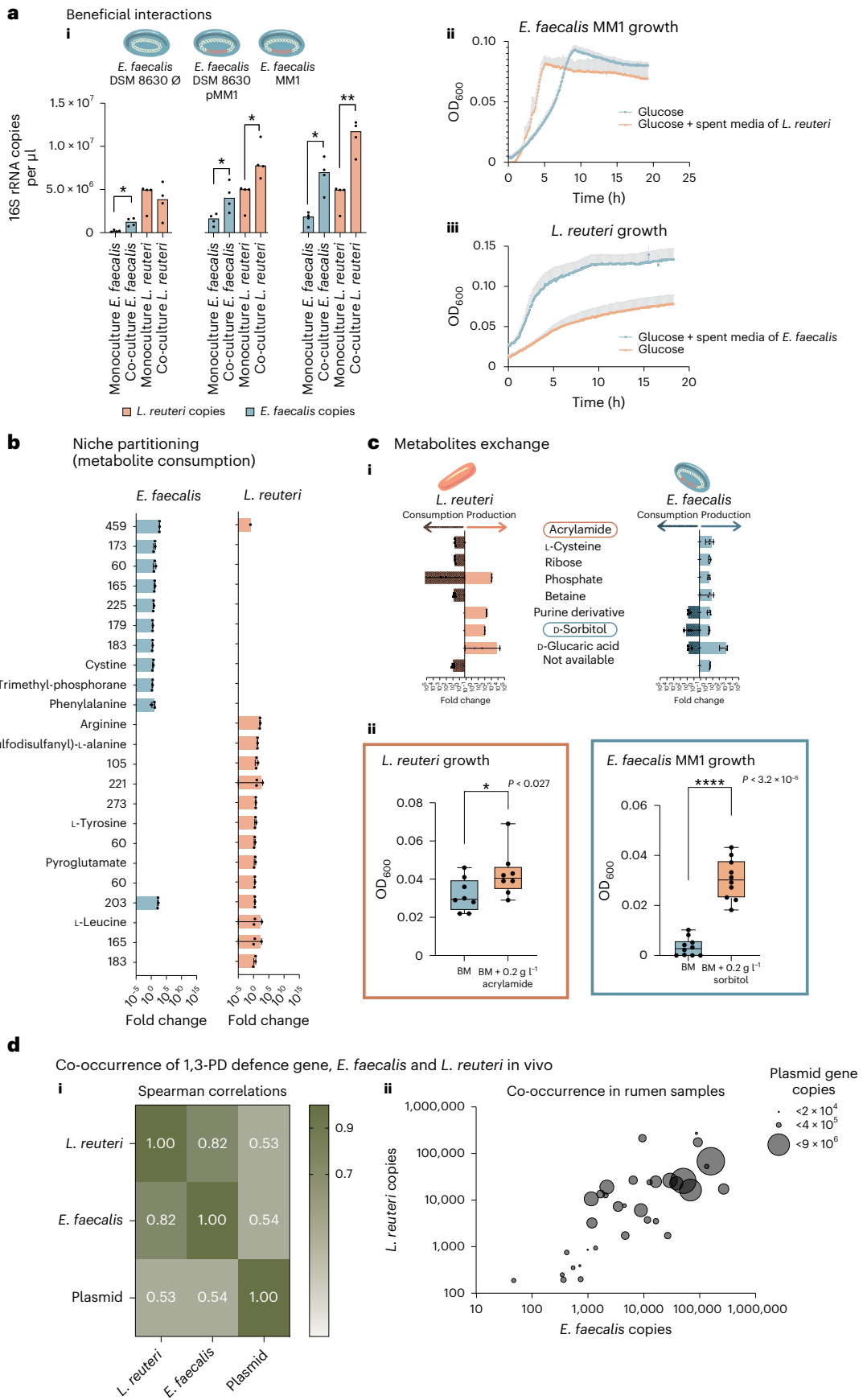
as a weapon when in close proximity. Indeed, when we co-cultured *E. faecalis* and *L. reuteri*, we identified a beneficial effect reflected in an increase in biomass of both species compared with the individual monocultures (Fig. 4a(i)). It is important to consider that in natural environments, microbial growth is often asynchronous³³ and reuterin may already be present during microbial interactions. Therefore, we externally added reuterin to our experiments to create controlled conditions that closely resemble the rumen environment, where reuterin is prevalent during the growth of both bacterial species as seen in our measurements of the rumen environment and in other gut environments^{34–37}. Our results demonstrate that in co-culture, the benefit on *L. reuteri* growth is observed only with *E. faecalis* strains containing 1,3-PD gene on plasmids and the benefit on *E. faecalis* growth is enhanced with the plasmid coding the 1,3-PD gene (Fig. 4a(i)). Proximity assays on solid media further corroborated these results; indeed, we observe an increase in the colony diameter of both *E. faecalis* and *L. reuteri* strains and a reduced distance between the two bacterial colonies only when the plasmidic 1,3-PD gene is present, allowing for increased beneficial interaction between the strains (Extended Data Fig. 6). Furthermore, when we cultured *E. faecalis* MM1 on *L. reuteri* spent growth media, we identified a significant increase in the generation time of *E. faecalis* when exposed to *L. reuteri* metabolites (Fig. 4a(ii)). Surprisingly, *L. reuteri* also showed a remarkable increase in fitness when exposed to *E. faecalis* metabolites (Fig. 4a(iii)), further suggesting that this interaction is dependent on metabolite exchange.

In view of the above, we performed an untargeted metabolomic analysis of production–consumption of metabolites of *E. faecalis* MM1 on spent medium of *L. reuteri* and vice versa (Supplementary Table 2). We detected a clear niche-partitioning pattern between the two microbes with regards to metabolite consumption, except for one metabolite consumed by both, suggesting that the two species are not competing for resources (Fig. 4b). Both microbes produce similar numbers of metabolites (Extended Data Fig. 7) and interestingly, the *E. faecalis* MM1 strain was able to consume 3 of the 52 metabolites identified to be produced by *L. reuteri*. Two of them were not present in the medium beforehand and were fully consumed by *E. faecalis* MM1. These metabolites could therefore be growth limiting and could potentially explain the faster growth of *E. faecalis* MM1 during the logarithmic stage on the spent media until they became limiting due to their total consumption and depletion by *E. faecalis* MM1. It should be noted that in the co-culture of both microbes, *E. faecalis* MM1 produces more biomass compared with its monoculture, potentially due to the higher availability of these metabolites under those conditions. Among the 41 metabolites produced by *E. faecalis* MM1, *L. reuteri* consumed 5, which were not fully consumed, thus explaining the higher biomass of this microbe grown on the spent medium, which corresponds to its growth in co-culture (Fig. 4a(iii)). In total, we annotated 29 metabolites out of the 84 metabolites of interest using five different platforms, some of which were reported in previous studies^{38–42} of *L. reuteri* and

Fig. 4 | Metabolic interaction between the reuterin producer and degrader.

a(i), Bar graph representing quantitative PCR analysis (16S rRNA gene) of mono- and co-cultures of *L. reuteri* (orange) with the different *E. faecalis* strains (blue) from 4 biological replicates using specific primers for each strain. Asterisks represent *P* values using two-sided *t*-test (values from left to right: 0.005, 0.027, 0.021, 0.003 and 0.001). (ii), (iii), Growth curves of *L. reuteri* (iii) or *E. faecalis* (ii) as represented by OD measured at 600 nm over time with and without *E. faecalis* or *L. reuteri* spent media. Mean + s.d. **b**, Bar graphs representing the fold change of the metabolites consumed by *L. reuteri* or *E. faecalis* cultured on basal defined medium as analysed by LC–MS. Fold changes of the consumed metabolites compared to the respective blank media are presented. **c**(i), Bar graphs displaying the fold change of the consumed and/or produced metabolites by each bacterial species. The analysis was carried out on samples cultured on spent medium obtained from the two strains on which they were grown reciprocally. All LC–MS measurements (in **b** and **c**) were performed on biological triplicates;

actual values (dots), mean \pm s.d. are presented. (ii), Boxplots representing supplementation assays with commercial acrylamide ($n = 8$) or sorbitol ($n = 10$) added to basal defined medium as the sole carbon source before growing *L. reuteri* or *E. faecalis*, respectively, for 20 h at 37 °C. All points are displayed and the means are represented as a line. Actual OD₆₀₀ values are displayed; *P* values obtained with two-sided *t*-test. Boxes represent the interquartile range (IQR) central half of the data, the whiskers indicate the range of the data, minimum to maximum values, and individual dots represent all the measurements. **d**, Co-occurrence of 1,3-PD gene, *E. faecalis* and *L. reuteri* in vivo. (i), Spearman correlations and (ii) co-occurrence scatterplot between the *L. reuteri*, *E. faecalis* and 1,3-PD gene abundances as determined by quantitative PCR using specific primers on 34 individual rumen samples. The *x* and *y* axes in ii represent the 16S rRNA gene copy number of *E. faecalis* and *L. reuteri*, respectively, and the circle sizes represent the 1,3-PD gene copy number.



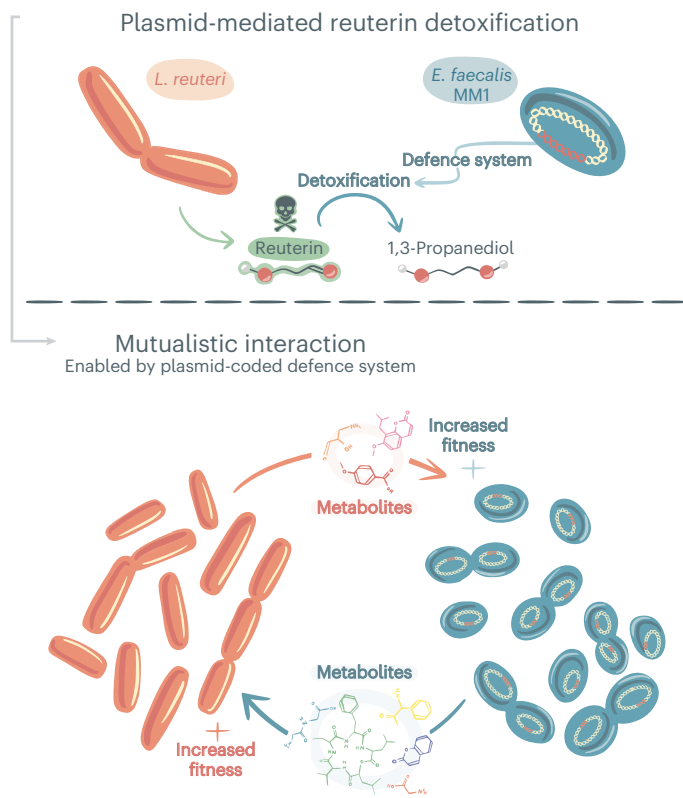


Fig. 5 | Schematic model of the findings revealed in our study. Our data demonstrate that the antibacterial toxin, reuterin, produced by *L. reuteri* (in orange) is detoxified by the plasmid-encoded defence gene (in red) of *E. faecalis* (in blue), thus allowing *E. faecalis* survival and use of *L. reuteri*-produced metabolites to increase its fitness. The beneficial effect becomes mutual when the metabolites produced by *E. faecalis* are consumed by *L. reuteri*, which in turn also increases the latter's fitness.

E. faecalis. The metabolites produced by *L. reuteri* and consumed by *E. faecalis* were annotated as D-sorbitol, D-glucaric acid and a purine metabolism derivative. Four out of the five metabolites produced by *E. faecalis* and consumed by *L. reuteri* were annotated as L-cysteine, ribose phosphate, acrylamide and betaine (Fig. 4c(i)). These annotations suggest that the two bacteria exchange metabolites that are not clustered in a specific pathway but spread across various pathways of their metabolism. We confirmed the annotations of acrylamide and D-sorbitol through LC-MS analysis using commercially available sources of these metabolites (Extended Data Fig. 8). Furthermore, we conducted growth experiments with *L. reuteri* and *E. faecalis* on acrylamide and D-sorbitol as the sole carbon sources, respectively, to confirm their utilization. Our results demonstrated that both bacterial strains were able to effectively utilize these compounds, resulting in positive effects on their growth (Fig. 4c(ii)). Altogether, our results suggest that metabolic exchange across the metabolic range between the two species is enabled by the maintenance of the defence plasmid coding for the 1,3-PD defence gene when reuterin is present in the environment (Fig. 5).

The observed beneficial interaction between *L. reuteri* and *E. faecalis* in vitro led us to investigate their relationship in vivo. We examined their co-occurrence and the presence of the 1,3-PD plasmidic gene in the rumen of 34 cows. Quantitative PCR analysis revealed a Spearman correlation of 0.82 between the two species (Fig. 4d(i)), and both *L. reuteri* and *E. faecalis* quantities were found to correlate with 1,3-PD plasmidic gene quantification, with Spearman correlations of 0.53 and 0.54, respectively (Fig. 4d(i)); fitting a linear regression model resulted in an R^2 of 0.6176 (Extended Data Fig. 9), indicating

that the observed beneficial interaction between these two species in vitro also occurs in natural environments (Fig. 4d(ii)). Moreover, an analysis of human gut plasmidomes from 311 faecal samples of healthy individuals revealed that 17% of the samples contained a plasmid with a putative 1,3-PD gene. This gene shared 44% amino-acid identity and 61% similarity to the rumen plasmid-borne 1,3-PD protein sequence. In addition, the putative 1,3-PD plasmid-borne gene was found to co-occur with *L. reuteri* (Fisher exact test, $P < 1 \times 10^{-5}$), indicating the widespread presence of this defence mechanism in gut environments where *L. reuteri* is present (Supplementary Table 3). These findings suggest that the observed in vitro interaction may be relevant in other gut environments as well.

Discussion

In dense microbial communities, such as gut ecosystems and specifically in rumen ecosystems, microbial weapons and defence mechanisms play an instrumental role in the establishment and maintenance of microbial interactions. Such interactions are mostly established by competing for resources such as space and nutrients. Most of the research on bacterial warfare has focused on the benefit or cost from the direct outcome of using the weapon or the defence system on the microbial population or on the type of interaction, for example, surviving the attack or winning the competition. Plasmids are thought to be instrumental in the dispersal of such systems and their effect on microbial communities. Nevertheless, there are only a few (if any) examples of indirect effects of such mechanisms for establishing or changing the type of interaction between the warring parties within the community.

Here we highlight a unique, higher-order beneficial interaction type that is dependent on and mediated by the implementation of a defence mechanism that is coded on a plasmid. This plasmid accessory function confers upon its bacterial host the ability to maintain a beneficial relationship with an attacking microbial species. The aim of our work was to gain deep insight into how plasmids containing accessory genes can influence the ecology within their ecosystem. Focusing on the rumen ecosystem, we identified a plasmid carrying the 1,3-PD accessory gene that has high occupancy across ecosystems, and we performed an integrated top-down/bottom-up study involving bioinformatics, biochemical, molecular and cellular analyses. We found that carrying the plasmid provides the means to resist the toxic effect of reuterin in vitro and enabled *E. faecalis* to maintain a mutualistic metabolic interaction with *L. reuteri*, a toxin producer, thereby contributing to the fitness of both parties. Both the reuterin producer and the reuterin degrader were able to consume the produced metabolites of its counterpart, which suggests reciprocity among these cross-feeding bacterial species. Conferring an advantage that is specific only for the bacterial host of the plasmid would also account for the absence of mobility genes on the plasmid, thereby providing exclusivity for the beneficial effect of the plasmid-borne defence system.

In addition to these ecological implications, it seems that the high prevalence of the reuterin defence system on a plasmid would designate reuterin as an antibacterial toxin that has noticeable ecological significance and relevance in the rumen ecosystem, as well as gut ecosystems in other animal species. We find circumstantial evidence to support this notion as we observed the occurrence of this plasmidic gene in natural rumen samples with a positive correlation to both *E. faecalis* and *L. reuteri*, suggesting a potential mutually beneficial interaction in vivo. Furthermore, we found a homologous plasmidic 1,3-PD gene to be widespread in human gut environments where *L. reuteri* is present, indicating the potential for such interactions to occur in human gut microbiota. Nevertheless, such correlations should be further investigated to confirm in vivo interactions between these species. Hence future studies are needed to strengthen our primary findings and to decipher the importance of such interactions in vivo while focusing on the spatial organization of the

interacting partners. The evolution of the toxin and defence gene in *L. reuteri* and *E. faecalis* is probably not driven by its role in enabling the interaction between these species. The production of reuterin has probably evolved primarily as a competitive mechanism, given its broad-spectrum toxin properties. The acquisition of the plasmid by *E. faecalis* may have occurred coincidentally along with its carried defence activity. Regardless of the chronological order of events, the presence of the defence system allows these two niche-partitioning non-competitive species to co-exist and support one another while excluding competitors.

To summarize, our findings show that a plasmid-coded trait has an important ecological role that is instrumental in bacterial warfare and interactions. They highlight the potential role of plasmids in facilitating mutualistic interactions between microbial species and emphasize plasmids' importance as drivers of community dynamics and interactions. Our results surface a conceptual paradigm in microbial war and peace, perhaps analogous to an arms race in human societies, whereby possession of a defence system by one partner against the weapons system of another would enable a status quo of peace and prosperity.

Methods

Bioinformatic analysis of 1,3-PD-associated plasmid

The plasmidomes of 78 Holstein dairy cows were retrieved from the raw reads of sequenced metagenomes¹⁶ using the Recycler algorithm¹⁷. Plasmid containing 1,3-PD genes was retrieved using local Blast⁴³. The plasmid was analysed for the presence of conjugative systems and relaxases using ConJScan⁴⁴ of McSyFinder and MOBscan⁴⁵. The raw reads of 311 healthy human individual faecal samples from project SRP100518 were trimmed using Trim Galore⁴⁶, assembled into contigs by Mega-hit⁴⁷ and plasmids were recovered by SCAPP⁴⁸. Next, the amino-acid sequence of the 1,3-PD gene from the rumen plasmidome was blasted against these plasmids, resulting in the retrieval of a plasmid encoding a putative 1,3-PD gene with 44% amino-acid identity and 61% similarity to the rumen plasmidome 1,3-PD protein sequence. Finally, raw reads of each of the 311 samples were mapped to this plasmid using BBmap⁴⁹, and the plasmid was considered present in a sample if its read coverage was higher than 70% as computed by SAMtools mpileup⁵⁰.

1,3-PD gene cloning and protein purification

The gene coding for 1,3-PD was synthesized and cloned into plasmid pSH21 such that the expressed protein presents an N-terminal poly-histidine tag (Supplementary Table 4). The resulting plasmid was inserted to *E. coli* ER2566 competent cells and the gene was expressed under the transcriptional control of the T7 promoter in the presence of 100 µg ml⁻¹ ampicillin. The protein was initially purified using Ni-NTA beads, followed by size exclusion chromatography using a GE Healthcare 16/60 Superdex 75 column that was equilibrated with 50 mM HEPES pH 7.5 and 100 mM NaCl. The purified protein was stored without glycerol at -80 °C.

Enzymatic activity of 1,3-PD

The putative enzyme performs the reaction 1,3-PD + NAD⁺ → NADH + reuterin and vice versa. Since purified reuterin is not commercially available, the enzymatic activity was measured using 1,3-propanediol and NAD⁺ as substrates. 1,3-Propanediol at 2 mM was used as a substrate in the presence of 1 mM NAD⁺ to measure the activity of the enzyme (1 µM). The absorbance at 340 nm was used to measure the production of NADH. The reaction was performed for 15 min at 37 °C. Kinetic parameters were determined via titration experiments by fitting a Michaelis–Menten model to the data.

Reuterin production by *L. reuteri*

The reuterin producer, *L. reuteri*, was used to produce reuterin from glycerol, as it converts glycerol to reuterin in the presence of glucose²⁴. *L. reuteri* strain ATCC 6475 was grown on MRS medium (Difco) under

anaerobic conditions for 24 h at 37 °C. The bacterial culture was then centrifuged under anaerobic conditions for 3 min at 5,000g. The supernatant was discarded, the cells were washed quickly with saline solution and resuspended in 1 ml of 250 mM glycerol, supplemented with 0.1% glucose and incubated at 37 °C for 2 h under anaerobic conditions. Then, after a centrifugation step at 12,000 g for 5 min, the aqueous supernatant containing the produced reuterin was filtered and kept at 4 °C. Aliquots of 50 µl of the supernatant or acrolein (Sigma-Aldrich) at concentrations ranging from 0 to 70 nM, or double-distilled water (negative control), were added to 37.5 µl tryptophan (0.01 M solution in 0.05 M HCl), together with 150 µl of concentrated HCl in 1.5 ml tubes, and the solution was incubated for 30 min at 37 °C. Absorbance, measured at 560 nm, was used to calculate the concentrations of reuterin produced by *L. reuteri*.

1,3-PD-based protection against reuterin

The gene coding for 1,3-PD was cloned into pBR322 using specific primers (Supplementary Table 4) using the Gibson assembly technique to form pBR322:1,3-PD. The plasmid was then transformed to *E. coli* ER2566 cells in the presence of 100 µg ml⁻¹ ampicillin. The plasmid pBR322 allows constitutive expression of the 1,3-PD gene. The wild-type strain ER2566 containing pBR322 alone and the ER2566 strain containing pBR322:1,3-PD were grown in 96-well plates with increasing concentrations of reuterin (0 to 1 mM) in 200 µl and incubated for 24 h at 37 °C (volumes of cultures were homogenized across samples using sterile water). Measurements of optical density (OD)_{600nm} after the incubation period were used to determine the protection against the reuterin compound by 1,3-PD. Similarly, *E. faecalis* MM1, DSM 8630 pMM1 and DSM 8630 ∅ were grown in increasing concentrations of reuterin (0 to 0.9 mM solution) in 1,000 µl of basal defined medium (volumes of cultures were homogenized across samples using sterile water), incubated at 37 °C for 24 h and measured for OD₆₀₀.

Preparation of reuterin standard

Three ml of reuterin produced by *L. reuteri* as described above was taken to prepare the reuterin standard using purification on a silica gel column as previously described⁵¹. The elution was monitored by adding a droplet of the eluent on a silica gel 60 thin-layer chromatography plate (Merck), which was immediately dipped into a 2% (w/v) Purpald reagent solution (Aldrich) in 1 M NaOH. Fractions with reuterin were combined and the solvent was evaporated under reduced pressure. The dry residue was weighed and immediately redissolved in double-distilled water to 2 mg ml⁻¹. The obtained solution was stored at -20 °C until preparation of the standard curve.

Measurement of reuterin

A number of 20 rumen samples taken from a previously published cow cohort¹⁶ were analysed for reuterin concentration using LC–MS. Reuterin was derivatized as previously described⁵² and analysed using an LC–MS/MS instrument consisting of an Acquity I-class UPLC system (Waters) and Xevo TQ-S triple quadrupole mass spectrometer (Waters) equipped with an electrospray ion source. MassLynx and TargetLynx software (v.4.2, Waters) were applied for the acquisition and analysis of data. Chromatographic separation was performed on a 50 mm × 2.1-mm-internal-diameter, 1.7-µm UPLC BEH C18 column (Waters Acquity), with 0.1% formic acid as mobile phase A and methanol as mobile phase B at a flow rate of 0.3 ml min⁻¹, and column temperature of 35 °C. A gradient was used as follows: a slight linear increase of B from 0.1 to 0.2% for 0–1.5 min; then a linear increase to 50% B for 5 min, held at 50% B for 0.5 min, back to 0.1% B within 0.5 min and equilibration at 0.1% B for 2 min. Injection volume was 3 µl.

Enrichment of reuterin-resistant bacteria

A cow sample in which the plasmid was detected was grown on M10 medium containing volatile fatty acids and supplemented with 5 g l⁻¹ fructose in liquid media and cultured via passaging for 7 d to reach

typical richness reduction resulting from growth in tubes. The bacterial community was further grown in the same medium (in 1 ml volumes, supplemented with 25 μ l reuterin (0.25 mM final concentration, which approximately corresponds to the average reuterin concentration detected in samples in which reuterin was present) or 25 μ l double-distilled water) and cultured by passaging for 7 d. The final cultures were observed under a light microscope and examined using in-house 16S rRNA gene-amplicon Illumina sequencing as previously described⁵³. An exact sequence variants table was created using DADA2 and QIIME^{54,55}.

Isolation of plasmid-containing bacteria

The supernatant fluids of the enriched culture above (containing various metabolites excreted by the community) were filtered using a 20- μ m-pore filter and used to enrich M10 agar plates containing volatile fatty acids and supplemented with 5 g l⁻¹ fructose. In addition, 0.1 mM reuterin was added to the plates to enrich for plasmid-containing bacteria. The obtained colonies were grown individually and subjected to miniprep preparation (RBC miniprep kit). Using specific primers for the 1,3-PD gene (Supplementary Table 1), PCR was performed on the purified plasmids using Phusion polymerase (NEB). Positive colonies were sent for 16S Sanger sequencing. To ensure the circular nature of the PCR product, all-around PCR was performed using the reverse complements of the specific 1,3-PD primers. The plasmid was then sequenced by Sanger sequencing and gene walking to fully validate the plasmid sequence.

Genomic comparison

The genomic DNA of *E. faecalis* DSM 8630 and MM1 strains was extracted using the phenol–chloroform method⁵⁶ and the DNA was sequenced using an Illumina sequencing NovaSeq S1. The sequences were assembled with SPAdes⁵⁷ and deposited in GenBank (accession numbers [JAMKBU000000000](https://www.ncbi.nlm.nih.gov/nuclseq/JAMKBU000000000) and [JAMKBV000000000](https://www.ncbi.nlm.nih.gov/nuclseq/JAMKBV000000000)).

The DNA contents of the two strains were compared using Mauve⁵⁸, and Proteinortho⁵⁹ was used to compare orthologous groups from both strains. A heat map of the orthologous group was created using Superheat in R (<https://ribarter.github.io/superheat/>).

CARD-FISH

Long probes (~300 bases) were designed for 1,3-PD and GroEL genes to perform standard CARD-FISH (Supplementary Table 4). PCR was performed using Ex Taq polymerase (TaKaRa) following manufacturer protocol and replacing 90% of the dTTP volume with Dig-11-dUTP (Merck).

Plasmids were stained using DNA CARD-FISH. All centrifugations were carried out at 5,000 g at room temperature for 5 min. *E. faecalis* MM1 or DSM 8630 strains were grown overnight in brain-heart infusion medium (Difco) at 37 °C and the pellets of 1 ml cultures were fixed with 4% paraformaldehyde for 15 min. Fixed cells were then centrifuged and permeabilized with lysis buffer containing 0.05 M EDTA pH 8, 0.1 M Tris-HCl pH 8 and lysozyme (Merck) at 3 mg ml⁻¹ in PBS. Lysis occurred at 4 °C for 15 min. Cells were then centrifuged before being resuspended in hybridization buffer (20% dextran sulfate, 20 mM Tris-HCl, 0.1% SDS, 0.8 M NaCl, 1% blocking reagent and 35% formamide). The reaction was incubated at 42 °C for 30 min and 5 μ M of the probe was added to the reaction. Cells were then placed at 95 °C for 10 min, incubated at 42 °C overnight and washed twice in hybridization buffer lacking formamide and dextran sulfate. The cells were then resuspended in antibody binding solution (1% Western blocking reagent in PBS, supplemented with 0.1% Pluronic F-68 reagent) and incubated for 45 min with rotation to block non-specific binding. Subsequently, 2 μ l of anti-digoxigenin-POD Fab fragments (Roche) was added and the cells were incubated for another 1.5 h. Cells were washed twice in PBS. The cell pellet was then resuspended in 100 μ l amplification solution (5 M NaCl, 20% dextran sulfate and 0.05%

Western blocking reagent solution in PBS). Then, 1 μ l 0.15% H₂O₂ and 0.1 μ l Alexa Fluor 647 Tyramide reagent (ThermoFisher) were added to the mixture, the cells were incubated at 37 °C for 45 min in the dark, following which, 1 ml PBS was added and the cells were centrifuged. Finally, the cells were washed twice in PBS and then counterstained with DAPI (1 μ g ml⁻¹). Images were acquired using a 3i Marianas spinning disk confocal microscope equipped with a Yokogawa W1 module and Prime 95B sCMOS camera. Excitation laser (absorbance 637 nm and emission filter 672–712 nm) was achieved using a \times 100 Zeiss Plan-Apochromat 1.4 NA DIC oil objective.

STORM

Stained *E. faecalis* MM1 cells (20 μ l) were immobilized on poly-L-lysine-treated STORM high glass-bottom 35-mm μ -Dish (ibidi, 81158) and imaged by direct STORM. Photoswitching of the Alexa 647 dye was induced by a STORM buffer: 7 μ M glucose oxidase (Sigma), 56 mM catalase (Sigma), 5 mM cysteamine (Sigma), 50 mM Tris, 10 mM NaCl and 10% glucose (pH 8)⁶⁰. Image acquisition and data reconstruction were performed using the Elyra PS1 system (\times 100 oil objective) and Zen software (Zeiss).

Genetic manipulation

Full-length plasmid from *E. faecalis* MM1 was cloned into pAM401 (ref. 61) into XbaI and SalI restriction sites and transformed into *E. faecalis* DSM 8630 competent cells by electroporation⁶², generating *E. faecalis* DSM 8630 pMM1. In parallel, pAM401 only was also transformed into *E. faecalis* DSM 8630 competent cells to serve as a negative control (*E. faecalis* DSM 8630 \emptyset).

Growth curves

E. faecalis MM1 or *L. reuteri* was grown at 37 °C in 0.2 ml basal defined medium for 20 h in 96-well plates in an OD plate reader (800TS absorbance reader, Biotek) under anaerobic conditions. Basal defined medium was prepared as described in Supplementary Table 5. All chemicals were ordered from Sigma-Aldrich, except for the amino acids (FORMEDIUM).

Mono- and co-cultures were performed by inoculating 100 μ l of fresh cultures in the same media in 8 ml volumes in Hungate tubes with addition of 0.25 mM reuterin, and incubating for 20 h at 37 °C. Given that *L. reuteri* produces reuterin during the late stationary phase, by including reuterin throughout the experiment, we aimed to mimic the conditions that more closely resemble the natural environment and the prevailing concentrations of reuterin in the rumen.

Supplementation assays were performed by adding 0.2 g l⁻¹ of acrylamide or sorbitol to basal defined medium without glucose before growing *L. reuteri* or *E. faecalis*, respectively, for 20 h at 37 °C. Acrylamide supplementation assays were performed in Hungate tubes to avoid acrylamide evaporation.

Quantitative PCR

Quantitative PCR was used to determine the copy number of the *E. faecalis* strains and *L. reuteri* in single and co-cultures. The pellets of 1 ml cultures were obtained by centrifugation at 4,000 g for 5 min and the genomic DNA was extracted as performed in ref. 56 without the initial filtration steps. A volume of 2 μ l of a 10-fold dilution was used in the reaction mix described below.

Standard curves suitable for the quantification of *Enterococcus*-specific and *L. reuteri* 16S rRNA genes were generated by amplifying serial 10-fold dilutions of quantified gel-extracted PCR products, obtained by amplification of each fragment (primers in Supplementary Table 4). The standard curves were obtained using 8 dilution points and were calculated using the Rotorgene 6000 series software (Qiagen). Real-time PCR was performed in a 10- μ l reaction mixture containing 5 μ l Absolute blue SYBR green master mix (Thermo Scientific), 0.5 μ l of each primer (at 10 mM) and 2 μ l of the DNA template.

Quantitative PCR was also used to determine the copy number of *E. faecalis*, *L. reuteri* and 1,3-PD genes in metagenomic DNA extracted from a cohort of 34 cows¹⁶. Copy numbers of each gene were normalized to the DNA concentration of each sample measured using a Qubit dsDNA High Sensitivity Assay kit (Invitrogen). The obtained plasmid quantities confirmed Recycler predictions and increased the detection level in additional samples. Linear regression was used to measure the relationship between the absolute abundance of *L. reuteri* and *E. faecalis* in these samples. The data were \log_{10} transformed before fitting the linear model with the `lm` function in R (v.4.2.1).

Proximity assay

Proximity assay was performed on 1-well plates containing basal defined medium supplemented with 1.5% agar with 0.25 mM reuterin. Plates were pre-incubated at room temperature for 24 h to avoid bacterial smears. *E. faecalis* and *L. reuteri* strains were spotted on the plates by depositing a volume of 2.5 μ l each at 1-cm distance and incubated at 37 °C for 48 h under anaerobic conditions. The assay was performed with either *E. faecalis* MM1, DSM 8630 pMM1 or DSM 8630 \emptyset .

After incubation, the distance between *L. reuteri* and *E. faecalis* colonies was measured, as well as the diameter of each colony.

Untargeted LC–MS analysis of metabolomes

E. faecalis MM1 was grown on basal defined medium alone or mixed with equal volumes of the spent medium of *L. reuteri* ATCC 6475 (0.2 ml total volume distributed in 96-well plates). Similarly, *L. reuteri* ATCC 6475 was grown for 24 h at 37 °C on basal defined medium alone or mixed with equal volumes of the spent medium of *E. faecalis* MM1. Supernatant fluids of all cultures were filter-sterilized for subsequent LC–MS analysis.

For metabolite extraction, a volume of 100 μ l from each supernatant fraction was mixed with 1 ml of pre-cooled metabolomics extraction mixture (methanol containing 2.5 μ g ml⁻¹ ampicillin). Tubes were incubated for 10 min in an orbital shaker before centrifugation at full speed for 10 min.

For polar metabolite analysis, 150 μ l of extracted metabolites or standards in LC–MS grade water was transferred to glass vials and kept at –20 °C until used. A volume of 5 μ l of each sample was injected into a C18 100 mm \times 2.1 mm \times 1.7 μ m reversed-phase column (Waters) using a Waters Acquity UPLC system. Mobile phases consisted of 0.1% formic acid (A), and acetonitrile supplemented with 0.1% formic acid (B) (UPLC MS grade, BioSolve). The metabolites were eluted at a flow rate of 400 μ l min⁻¹, using the following percentages of A: 1-min gradient from 99 to 95%; 7-min gradient from 95 to 1%; 2.9 min at 1%; 0.1-min gradient from 1 to 5%; 2-min gradient from 5 to 99%, and 2 min at 99% for washing and re-equilibration of the column (15 min total run time). The mass spectra were acquired using an Exactive mass spectrometer (ThermoFisher). The spectra were recorded using both full scan and all-ion fragmentation scan mode, covering a mass range of 100–1,500 *m/z*. The resolution was set to 70,000 with 10 scans per second, restricting the Orbitrap loading time to a maximum of 100 ms with a target value of 1×10^5 ions. The capillary voltage was set to 3.5 kV, with a sheath gas flow value of 60 and an auxiliary gas flow of 20. The capillary temperature was set at 275 °C, while the drying gas in the heated electrospray source was set at 300 °C. Chromatogram processing, peak detection and integration were performed using MZmine 2, with signal to noise ratio set to 5 (MZmine 2.41.2)⁶³. Production of metabolites was defined as a ratio of ‘metabolites after growth/metabolites before growth’ equal or superior to 2.5. Consumption of metabolites was defined as the same ratio equal or inferior to 0.4. To increase stringency, production or consumption of a metabolite was further confirmed if the metabolite was produced or consumed in three biological replicates. Metabolites that were neither produced nor consumed by *E. faecalis* or *L. reuteri* were ignored. Metabolite annotations were performed by matching masses

and retention times obtained by running the commercial Mass Spectrometry Metabolite Library of Standards (MSMLS, Iroa Technologies). Additional annotations were obtained by: performing Molecular Networking using GNPS⁶⁴, using the Compound Discoverer v.3.3 (Thermo Scientific), extracting the metabolites present in the KEGG genomes of the bacteria^{40,65} and using MetaboAnalyst⁶⁶. The latter tool was used to detect peaks that corresponded to the same compound with various ionizations. For these metabolites, we chose the ionized compound that was better detected as a representative peak.

Commercial acrylamide and D-sorbitol were purchased (Merck) to validate their annotations, using the workflow described above.

Statistics and reproducibility

No statistical method was used to predetermine sample size. No data were excluded from the analyses. The experiments were not randomized. Data distribution was assumed to be normal, but this was not formally tested (individual datapoints are presented in the figures). The Investigators were not blinded to allocation during experiments and outcome assessment.

Reporting summary

Further information on research design is available in the Nature Portfolio Reporting Summary linked to this article.

Data availability

Genome sequencing and 16S rRNA sequences of *E. faecalis* MM1 and DSM 8630 have been deposited in GenBank ([JAMKBV000000000](https://www.ncbi.nlm.nih.gov/GenBank/), [JAMKBV000000000](https://www.ncbi.nlm.nih.gov/GenBank/), [OR513053](https://www.ncbi.nlm.nih.gov/GenBank/) and [OR513080](https://www.ncbi.nlm.nih.gov/GenBank/)). Metabolomics data are deposited in MetaboLights⁶⁷ under the identifier MTBLS7248 (<https://www.ebi.ac.uk/metabolights/editor/MTBLS7248/descriptors>). Source data are provided with this paper.

References

- Kado, C. I. Origin and evolution of plasmids. *Antonie Van Leeuwenhoek* **73**, 117–126 (1998).
- Heuer, H., Abdo, Z. & Smalla, K. Patchy distribution of flexible genetic elements in bacterial populations mediates robustness to environmental uncertainty. *FEMS Microbiol. Ecol.* **65**, 361–371 (2008).
- Nuti, M. P., Lepidi, A. A., Prakash, R. K., Hooykaas, P. J. J. & Schilperoord, R. A. in *Molecular Biology of Plant Tumors* (eds Kahl, G. & Schell, J. S.) 561–588 (Academic Press, 1982).
- Zwanzig, M. The ecology of plasmid-coded antibiotic resistance: a basic framework for experimental research and modeling. *Comput. Struct. Biotechnol. J.* **19**, 586–599 (2021).
- Frost, L. S., Leplae, R., Summers, A. O. & Toussaint, A. Mobile genetic elements: the agents of open source evolution. *Nat. Rev. Microbiol.* **3**, 722–732 (2005).
- Novick, R. P. Mobile genetic elements and bacterial toxinoses: the superantigen-encoding pathogenicity islands of *Staphylococcus aureus*. *Plasmid* **49**, 93–105 (2003).
- Crossman, L. C. Plasmid replicons of *Rhizobium*. *Biochem. Soc. Trans.* **33**, 157–158 (2005).
- van der Meer, J. R. & Sentchilo, V. Genomic islands and the evolution of catabolic pathways in bacteria. *Curr. Opin. Biotechnol.* **14**, 248–254 (2003).
- Gil, R., Sabater-Muñoz, B., Perez-Brocá, V., Silva, F. J. & Latorre, A. Plasmids in the aphid endosymbiont *Buchnera aphidicola* with the smallest genomes. A puzzling evolutionary story. *Gene* **370**, 17–25 (2006).
- Shterzer, N. & Mizrahi, I. The animal gut as a melting pot for horizontal gene transfer. *Can. J. Microbiol.* **61**, 603–605 (2015).
- Granato, E. T., Meiller-Legrand, T. A. & Foster, K. R. The evolution and ecology of bacterial warfare. *Curr. Biol.* **29**, R521–R537 (2019).

12. Morais, S. & Mizrahi, I. Islands in the stream: from individual to communal fiber degradation in the rumen ecosystem. *FEMS Rev. Microbiol.* **43**, 362–379 (2019).
13. Mizrahi, I., Wallace, R. J. & Morais, S. The rumen microbiome: balancing food security and environmental impacts. *Nat. Rev. Microbiol.* **19**, 553–566 (2021).
14. Kav, A. B. et al. Insights into the bovine rumen plasmidome. *Proc. Natl Acad. Sci. USA* **109**, 5452–5457 (2012).
15. Brown Kav, A. et al. Unravelling plasmidome distribution and interaction with its hosting microbiome. *Environ. Microbiol.* **22**, 32–44 (2020).
16. Shabat, S. K. B. et al. Specific microbiome-dependent mechanisms underlie the energy harvest efficiency of ruminants. *ISME J.* **10**, 2958–2972 (2016).
17. Rozov, R. et al. Recycler: an algorithm for detecting plasmids from de novo assembly graphs. *Bioinformatics* **33**, 475–482 (2017).
18. Shapiro, J. T. et al. Multilayer networks of plasmid genetic similarity reveal potential pathways of gene transmission. *ISME J.* **17**, 649–659 (2023).
19. Brown Kav, A., Benhar, I. & Mizrahi, I. A method for purifying high quality and high yield plasmid DNA for metagenomic and deep sequencing approaches. *J. Microbiol. Methods* **95**, 272–279 (2013).
20. Humphrey, S. et al. Staphylococcal phages and pathogenicity islands drive plasmid evolution. *Nat. Commun.* **12**, 5845 (2021).
21. Frickey, T. & Lupas, A. N. PhyloGenie: automated phylome generation and analysis. *Nucleic Acids Res.* **32**, 5231–5238 (2004).
22. Raynaud, C., Sarçabal, P., Meynial-Salles, I., Croux, C. & Soucaille, P. Molecular characterization of the 1,3-propanediol (1,3-PD) operon of *Clostridium butyricum*. *Proc. Natl Acad. Sci. USA* **100**, 5010–5015 (2003).
23. Smillie, C., Garcillán-Barcia, M. P., Francia, M. V., Rocha Eduardo, P. C. & de la Cruz, F. Mobility of plasmids. *Microbiol. Mol. Biol. Rev.* **74**, 434–452 (2010).
24. Talarico, T. L., Casas, I. A., Chung, T. C. & Dobrogosz, W. J. Production and isolation of reuterin, a growth inhibitor produced by *Lactobacillus reuteri*. *Antimicrob. Agents Chemother.* **32**, 1854–1858 (1988).
25. Degnan, P. H., Taga, M. E. & Goodman, A. L. Vitamin B12 as a modulator of gut microbial ecology. *Cell Metab.* **20**, 769–778 (2014).
26. Daniel, R., Boenigk, R. & Gottschalk, G. Purification of 1,3-propanediol dehydrogenase from *Citrobacter freundii* and cloning, sequencing, and overexpression of the corresponding gene in *Escherichia coli*. *J. Bacteriol.* **177**, 2151–2156 (1995).
27. Marçal, D., Rêgo, A. T., Carrondo, M. A. & Enguita, F. J. 1,3-propanediol dehydrogenase from *Klebsiella pneumoniae*: decameric quaternary structure and possible subunit cooperativity. *J. Bacteriol.* **191**, 1143–1151 (2009).
28. Luers, F., Seyfried, M., Daniel, R. & Gottschalk, G. Glycerol conversion to 1,3-propanediol by *Clostridium pasteurianum*: cloning and expression of the gene encoding 1,3-propanediol dehydrogenase. *FEMS Microbiol. Lett.* **154**, 337–345 (1997).
29. Johnson, E. A. & Lin, E. C. *Klebsiella pneumoniae* 1,3-propanediol: NAD⁺ oxidoreductase. *J. Bacteriol.* **169**, 2050–2054 (1987).
30. Cleusix, V., Lacroix, C., Vollenweider, S., Duboux, M. & Le Blay, G. Inhibitory activity spectrum of reuterin produced by *Lactobacillus reuteri* against intestinal bacteria. *BMC Microbiol.* **7**, 101 (2007).
31. Goris, J. et al. DNA-DNA hybridization values and their relationship to whole-genome sequence similarities. *Int. J. Syst. Evol. Microbiol.* **57**, 81–91 (2007).
32. Fautin, D. G. The anemonefish symbiosis: what is known and what is not. *Symbiosis* **10**, 23–46 (1991).
33. Korem, T. et al. Growth dynamics of gut microbiota in health and disease inferred from single metagenomic samples. *Science* **349**, 1101–1106 (2015).
34. Castellani, C. et al. Production, storage stability, and susceptibility testing of reuterin and its impact on the murine fecal microbiome and volatile organic compound profile. *Front. Microbiol.* **12**, 699858 (2021).
35. Zhang, J., Sturla, S., Lacroix, C. & Schwab, C. Gut microbial glycerol metabolism as an endogenous acrolein source. *mBio* **9**, e01947-17 (2018).
36. Engels, C. et al. Acrolein contributes strongly to antimicrobial and heterocyclic amine transformation activities of reuterin. *Sci. Rep.* **6**, 36246 (2016).
37. Morita, H. et al. Comparative genome analysis of *Lactobacillus reuteri* and *Lactobacillus fermentum* reveal a genomic island for reuterin and cobalamin production. *DNA Res.* **15**, 151–161 (2008).
38. Keogh, D. et al. Enterococcal metabolite cues facilitate inter-species niche modulation and polymicrobial infection. *Cell Host Microbe* **20**, 493–503 (2016).
39. Ryu, H. W. & Wee, Y. J. Characterization of bioconversion of fumarate to succinate by alginate immobilized *Enterococcus faecalis* RKY1. *Appl. Biochem. Biotechnol.* **91–93**, 525–535 (2001).
40. Pérez Escriba, P., Fuhrer, T. & Sauer, U. Distinct N and C cross-feeding networks in a synthetic mouse gut consortium. *mSystems* **7**, e0148421 (2022).
41. Kaneuchi, C., Seki, M. & Komagata, K. Production of succinic acid from citric acid and related acids by *Lactobacillus* strains. *Appl. Environ. Microbiol.* **54**, 3053–3056 (1988).
42. Kristjansdottir, T. et al. A metabolic reconstruction of *Lactobacillus reuteri* JCM 1112 and analysis of its potential as a cell factory. *Microb. Cell Fact.* **18**, 186 (2019).
43. Altschul, S. F. et al. Gapped BLAST and PSI-BLAST: a new generation of protein database search programs. *Nucleic Acids Res.* **25**, 3389–3402 (1997).
44. Cury, J., Abby, S. S., Doppelt-Azeroual, O., Néron, B. & Rocha, E. P. C. Identifying conjugative plasmids and integrative conjugative elements with CONJscan. *Methods Mol. Biol.* **2075**, 265–283 (2020).
45. Garcillán-Barcia, M. P., Redondo-Salvo, S., Vielva, L. & de la Cruz, F. MOBscan: automated annotation of MOB relaxases. *Methods Mol. Biol.* **2075**, 295–308 (2020).
46. Krueger, F. et al. FelixKrueger/TrimGalore: v0.6.10 - add default decompression path (0.6.10). Zenodo <https://doi.org/10.5281/zenodo.7598955> (2023).
47. Li, D., Liu, C.-M., Luo, R., Sadakane, K. & Lam, T.-W. MEGAHIT: an ultra-fast single-node solution for large and complex metagenomics assembly via succinct de Bruijn graph. *Bioinformatics* **31**, 1674–1676 (2015).
48. Pellow, D. et al. SCAPP: an algorithm for improved plasmid assembly in metagenomes. *Microbiome* **9**, 144 (2021).
49. Bushnell, B. *BBMap: A Fast, Accurate, Splice-aware Aligner*. No. LBNL-7065E (Ernest Orlando Lawrence Berkeley National Laboratory, 2014).
50. Li, H. et al. The Sequence Alignment/Map format and SAMtools. *Bioinformatics* **25**, 2078–2079 (2009).
51. Vollenweider, S., Grassi, G., König, I. & Puhán, Z. Purification and structural characterization of 3-hydroxypropionaldehyde and its derivatives. *J. Agric. Food Chem.* **51**, 3287–3293 (2003).
52. Yasuo, M. et al. The relationship between acrolein and oxidative stress in COPD: in systemic plasma and in local lung tissue. *Int. J. Chron. Obstruct. Pulmon. Dis.* **14**, 1527–1537 (2019).
53. Furman, O. et al. Stochasticity constrained by deterministic effects of diet and age drive rumen microbiome assembly dynamics. *Nat. Commun.* **11**, 1904 (2020).
54. Caporaso, J. G. et al. QIIME allows analysis of high-throughput community sequencing data. *Nat. Methods* **7**, 335–336 (2010).
55. Callahan, B. J. et al. DADA2: high-resolution sample inference from Illumina amplicon data. *Nat. Methods* **13**, 581–583 (2016).

56. Stevenson, D. M. & Weimer, P. J. Dominance of *Prevotella* and low abundance of classical ruminal bacterial species in the bovine rumen revealed by relative quantification real-time PCR. *Appl. Microbiol. Biotechnol.* **75**, 165–174 (2007).
57. Bankevich, A. et al. SPAdes: a new genome assembly algorithm and its applications to single-cell sequencing. *J. Comput. Biol.* **19**, 455–477 (2012).
58. Darling, A. C. E., Mau, B., Blattner, F. R. & Perna, N. T. Mauve: multiple alignment of conserved genomic sequence with rearrangements. *Genome Res.* **14**, 1394–1403 (2004).
59. Lechner, M. et al. Proteinortho: detection of (co-)orthologs in large-scale analysis. *BMC Bioinformatics* **12**, 124 (2011).
60. Goliand, I. et al. Resolving ESCRT-III spirals at the intercellular bridge of dividing cells using 3D STORM. *Cell Rep.* **24**, 1756–1764 (2018).
61. Fujimoto, S. & Ike, Y. pAM401-based shuttle vectors that enable overexpression of promoterless genes and one-step purification of tag fusion proteins directly from *Enterococcus faecalis*. *Appl. Environ. Microbiol.* **67**, 1262–1267 (2001).
62. Holo, H. & Nes, I. F. High-frequency transformation, by electroporation, of *Lactococcus lactis* subsp. *cremoris* grown with glycine in osmotically stabilized media. *Appl. Environ. Microbiol.* **55**, 3119–3123 (1989).
63. Pluskal, T., Castillo, S., Villar-Briones, A. & Oresic, M. MZmine 2: modular framework for processing, visualizing, and analyzing mass spectrometry-based molecular profile data. *BMC Bioinformatics* **11**, 395 (2010).
64. Wang, M. et al. Sharing and community curation of mass spectrometry data with Global Natural Products Social Molecular Networking. *Nat. Biotechnol.* **34**, 828–837 (2016).
65. Vieira-Silva, S. et al. Species–function relationships shape ecological properties of the human gut microbiome. *Nat. Microbiol.* **1**, 16088 (2016).
66. Pang, Z. et al. Using MetaboAnalyst 5.0 for LC–HRMS spectra processing, multi-omics integration and covariate adjustment of global metabolomics data. *Nat. Protoc.* **17**, 1735–1761 (2022).
67. Haug, K. et al. MetaboLights: a resource evolving in response to the needs of its scientific community. *Nucleic Acids Res.* **48**, D440–D444 (2020).

Acknowledgements

This work was funded by the DIP (2476/2 -1) and ERC (866530) to I.M. Funding was also provided by ISF (1947/19) to I.M. and S.M. We thank O. X. Cordero (Massachusetts Institute of Technology, USA), E. A. Bayer (Weizmann Institute of Sciences, Israel) and E. Jami (Agricultural Research Organization, Israel) for critically proofreading the manuscript; D. Perlman for the beautiful artwork; I. Amit for technical work; and the Ilse Katz Institute for Nanoscale Science and Technology Shared Resource Facility under the direction of U. Hadad for image acquisition with the spinning disk confocal microscope.

Author contributions

S.M. and I.M. jointly designed the experiments, analysed the data and wrote the paper. S.M. performed the experiments with technical help from M.M. A.Z. and D.B. performed bioinformatics analysis of the plasmidomes. M.I. and E.G. performed biochemical characterization of the 1,3-PD gene. J.W. provided expertise on reuterin production and critically read the paper. O.T.-H. and T.Z. contributed to metabolomic data analysis. A.B. performed targeted LC–MS of rumen samples. N.E. conducted STORM experiments and analysed the data. I.M. secured funding, supervised the work and synthesized the results.

Competing interests

The authors declare no competing interests.

Additional information

Extended data is available for this paper at <https://doi.org/10.1038/s41564-023-01521-9>.

Supplementary information The online version contains supplementary material available at <https://doi.org/10.1038/s41564-023-01521-9>.

Correspondence and requests for materials should be addressed to Itzhak Mizrahi.

Peer review information *Nature Microbiology* thanks the anonymous reviewers for their contribution to the peer review of this work.

Reprints and permissions information is available at www.nature.com/reprints.

Publisher's note Springer Nature remains neutral with regard to jurisdictional claims in published maps and institutional affiliations.

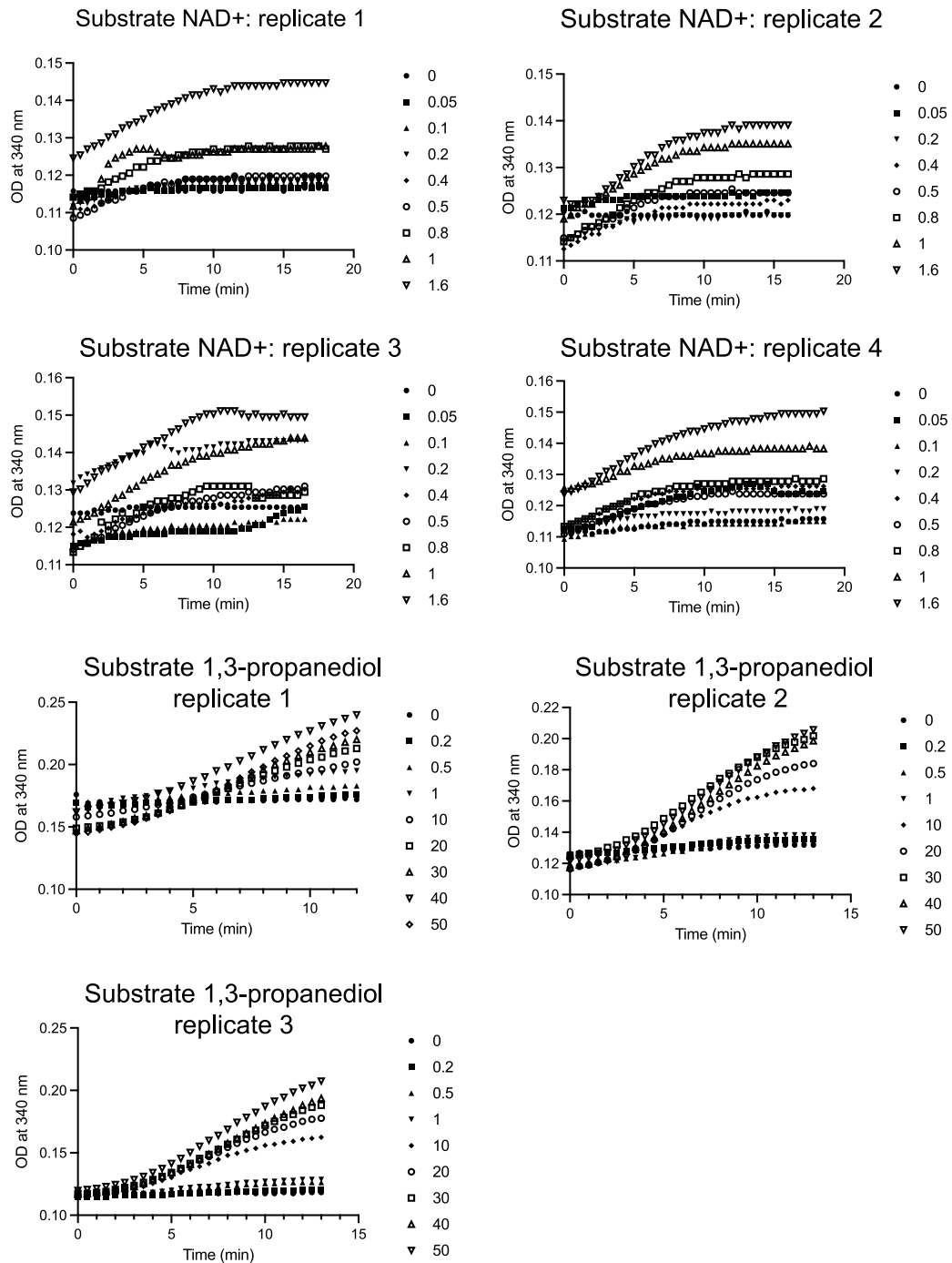
Open Access This article is licensed under a Creative Commons Attribution 4.0 International License, which permits use, sharing, adaptation, distribution and reproduction in any medium or format, as long as you give appropriate credit to the original author(s) and the source, provide a link to the Creative Commons license, and indicate if changes were made. The images or other third party material in this article are included in the article's Creative Commons license, unless indicated otherwise in a credit line to the material. If material is not included in the article's Creative Commons license and your intended use is not permitted by statutory regulation or exceeds the permitted use, you will need to obtain permission directly from the copyright holder. To view a copy of this license, visit <http://creativecommons.org/licenses/by/4.0/>.

© The Author(s) 2023

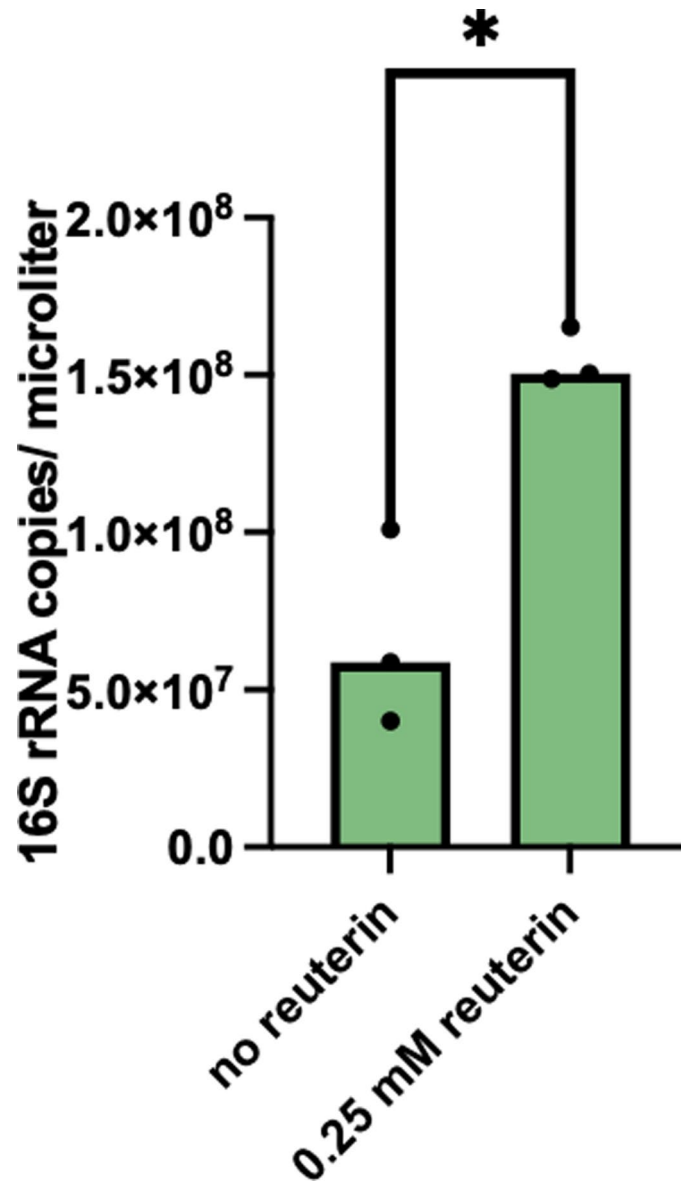
CLUSTAL O(1.2.4) multiple sequence alignment

1,3-PD_Thermotoga_maritima	----MWEFYMPTDVFVFGKILEKRGNIIDLLGKR-ALVVTG-KSSSKKNGSLDDLKLLD	54
1,3-PD_rumen_plasmidome	--MRYYDFLNPSVNFMGPNCEVLLGERCQILGMNKPMIVTDGFLASMENGPVAQSVASLE	58
1,3-PD_Klebsiella_pneumoniae	MSYRMFDYLVPNVNFPGNAISVVGERCQLLGGKKALLVTDKGLRAIKDGAVDKTLHYLR	60
1,3-PD_Citrobacter_freundii	MSYRMFDYLVPNVNFPGNAISVVGERCQLLGGKKALLVTDKGLRAIKDGAVDKTLHYLR	60
1,3-PD_Clostridium_pasteurianum	--MRMYDFLAPNVNFMGAGAIKLVGERCKILGGKKALIVTDKFLRNMEDGAVAQTVKYIK	58
1,3-PD_Clostridium_butyricum	--MRMYDYLVPSVNFMGANSVSVVGERCKILGGKKALIVTDKFLKDMEGGAVELTVKYLK	58
	::: * : ** : : * : ** : ** : : :	
1,3-PD_Thermotoga_maritima	ETEISYEIFDEVEENPSFDNVMKAVERYRNSDFVVLGGGSPMDFAKAVAVLLKEKDL	114
1,3-PD_rumen_plasmidome	KAGIEYVIFTGVEPNPKIQNCYSGLEMYKAEGCDSIITVGGGSAHDCGKIGIVATHD--	116
1,3-PD_Klebsiella_pneumoniae	EAGIEVAIFDGVPEPNKDTNVRDGLAVFRREQCDDIIVTVGGGSPHDCGKIGIAATHE--	118
1,3-PD_Citrobacter_freundii	EAGIDVVVFDGVPEPNKDTNVRDGLVFRKEHCDDIIVTVGGGSPHDCGKIGIAATHE--	118
1,3-PD_Clostridium_pasteurianum	EAGIDVAFYDDVEPNPKDTNVRDGLKVYRKENCDLIVTVGGGSSHDCGKIGIAATHE--	116
1,3-PD_Clostridium_butyricum	EAGLDVYYDGVPEPNKDVNIEGLKIFKEENCDMIVTVGGGSSHDCGKIGIAATHE--	116
	::: : ** * : : : * : : * : ** * : * : * : *	
1,3-PD_Thermotoga_maritima	SVEDLYDRE----KVKHWLPVVEIPTTAGTGVSEVTPYSILTDPEGNKRGCTL---MFPVY	167
1,3-PD_rumen_plasmidome	--GNIAEYAGIEKLTNALPPIVAVNTTAGTASEVTRHCVLTNADTKLKFVIVSWRNPLV	174
1,3-PD_Klebsiella_pneumoniae	--GDLYQYAGIETLTNPLPPIVAVNTTAGTASEVTRHCVLNTETKVKFVIVSWRNPLSV	176
1,3-PD_Citrobacter_freundii	--GDLYSYAGIETLTNPLPPIVAVNTTAGTASEVTRHCVLNTTKTKVKFVIVSWRNPLSV	176
1,3-PD_Clostridium_pasteurianum	--GDLYDYAGIETLTNPLPPIVAVNTTAGTGVSEVTRHCVITNTKTKIKFVIVSWRNPLV	174
1,3-PD_Clostridium_butyricum	--GDLYDYAGIETLVNPLPPIVAVNTTAGTASELTRHCVLNTKTKIKFVIVSWRNPLV	174
	:: : : * : ** * : * : * : * : * : * : * : *	
1,3-PD_Thermotoga_maritima	AFLDPRYTYSMSDELTLSTGVDALSHAVEGYLSRKSTPPSDALAIEAMKIIHRNLPKAI-	226
1,3-PD_rumen_plasmidome	SFNDPMLMLEVPAGLTAATGMDALTHAIETYVSDANPVTDAVAIQAIKLISGNLRQAVA	234
1,3-PD_Klebsiella_pneumoniae	SINDPMLMIGKPAALTAATGMDALTHAVEAYISKDANPVTDAAMQAIIRLIARNLRQAVA	236
1,3-PD_Citrobacter_freundii	SINDPMLMIGKPAALTAATGMDALTHAVEAYISKDANPVTDAAMQAIIRLIARNLRQAVA	236
1,3-PD_Clostridium_pasteurianum	SINDPILMIKKPAGLTAATGMDALTHAIESYVSKDANPVTDAIAIQAIKLINLRQAVA	234
1,3-PD_Clostridium_butyricum	SINDPMLMVKKPAGLTAATGMDALTHAIEYVSKDANPVTDAIAIQAIKLISQNLQAVA	234
	:: ** ** : ** * : * : * : * : * : * : * : *	
1,3-PD_Thermotoga_maritima	-EGNREARKMFVASCLAGMVIQTGTTLAHALGYPLTTEKGIKHGKATGMVLPFVMEVM	285
1,3-PD_rumen_plasmidome	NGYNVEARENMAYGSLLAGMAFNNGNLGYVHAMAHQLGGQYDMPHGVANAMLLPVVEEFN	294
1,3-PD_Klebsiella_pneumoniae	LGSNLQAREYMAYASLLAGMAFNANLGYVHAMAHQLGGYDMPHGVANAVLLPHVARYN	296
1,3-PD_Citrobacter_freundii	LGSNLKARENMAYASLLAGMAFNANLGYVHAMAHQLGGYDMPHGVANAVLLPHVARYN296	
1,3-PD_Clostridium_pasteurianum	LGENLEARENMAYASLLAGMAFNANLGYVHAMAHQLGGLYDMAHGVANAMLLPHVERYN	294
1,3-PD_Clostridium_butyricum	LGENLEARENMAYASLLAGMAFNANLGYVHAMAHQLGGLYDMPHGVANAMLLPHVERYN	294
	* : ** * : * : ** * : * : * : * : * : * : *	
1,3-PD_Thermotoga_maritima	KEEIEPEKVDTVNHIFGSSLLKFI-----LKELGLYEK--VAVSSEELEK	326
1,3-PD_rumen_plasmidome	MISNPQKFADIAEFMGVNTTEGLSTMAAADKAITAMRRLATDVGIPITSLKEMGVKEEDFDL	354
1,3-PD_Klebsiella_pneumoniae	LIANPEKFADIAELMGENITGLSTLDAAEKAIATRLSMDIGIPQHLRDLGVKETFDFPY	356
1,3-PD_Citrobacter_freundii	LIANPEKFADIAEFMGENTDGLSTMDAAELAIHAIARLSADIGIPQHLRDLGVKEADFPY	356
1,3-PD_Clostridium_pasteurianum	LISNPKKFADIAEFMGENIEGLSVMEAAEKAIAMFRLSKDVGIPASLKEMGVNEGDFEY	354
1,3-PD_Clostridium_butyricum	MLSNPKKFADIAEFMGENISGLSVMEAAEKAINAMFRLSEDVGIPKSLKEMGVKQEDFEH	354
	* : * : * : * : : : * : * : * : * : *	
1,3-PD_Thermotoga_maritima	WVEKGSRAKHLKNTPTGFTPEKIRNIYREALGV	359
1,3-PD_rumen_plasmidome	MATNALLDGNAGSNPRKGTQDIINLFKKAY--	385
1,3-PD_Klebsiella_pneumoniae	MAEMALKDGNAFSNPRKGNEQEIAAIFRQAF--	387
1,3-PD_Citrobacter_freundii	MAEMALKDGNAFSNPRKGNEKEIAEIFRQAF--	387
1,3-PD_Clostridium_pasteurianum	MAKMALKDGNAFSNPRKGNEKDIVKIFREAF--	385
1,3-PD_Clostridium_butyricum	MAELALLDGNAFSNPRKGNAKDIINIFKAAY--	385
	:: : : * : * : * : * : *	

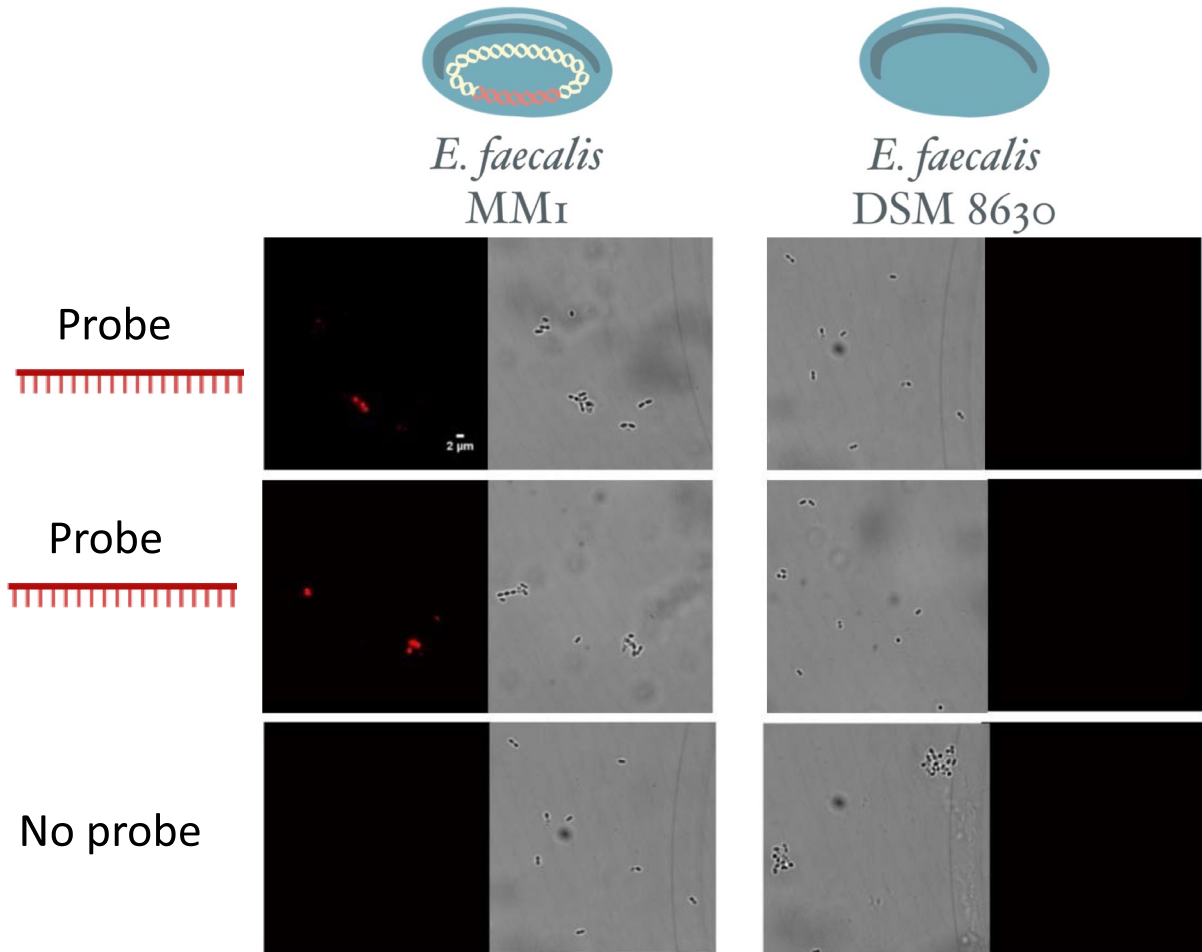
Extended Data Fig. Fig. 1 | Multiple sequence alignment of 1,3-PD genes. Amino-acid sequence alignment of the putative rumen plasmid 1,3-PD gene variant shows high similarities with other previously characterized enzymes from this family.



Extended Data Fig. 2 | Measurements of 1-3 PD kinetics. Each graph depicts a representative replicate of the absorbance at 340 nm measured over time at the indicated concentrations of NAD⁺ or 1,3-PD at increasing concentrations.

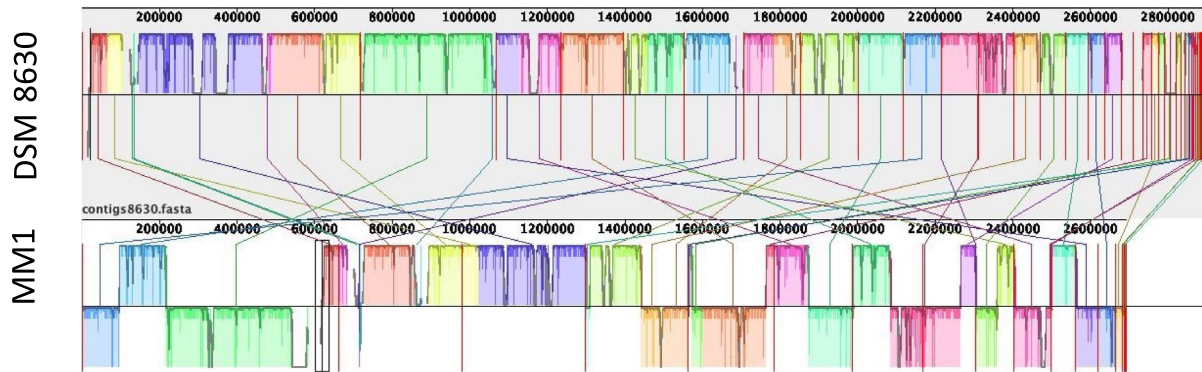


Extended Data Fig. 3 | Effect of reuterin on rumen microcosms biomass. The 16S rRNA copies of the microcosms are given for three biological triplicates (actual values are indicated). Asterisk represents *P* value of 0.009 with two-sided t-test without adjustment for multiple comparisons.

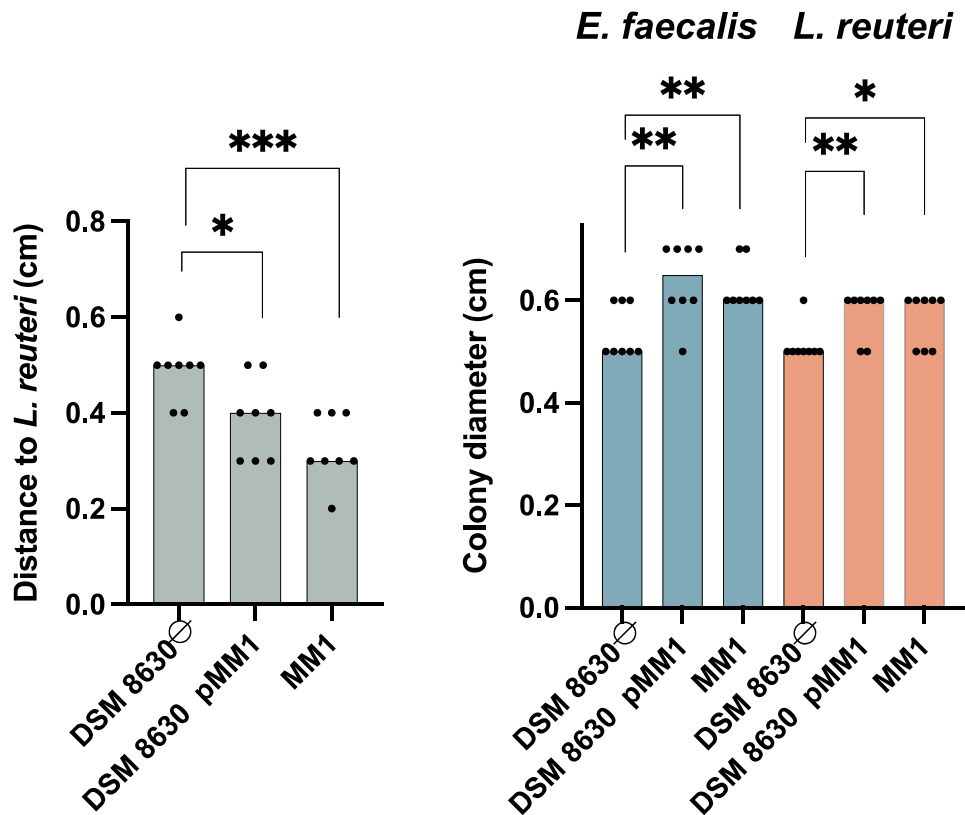


Extended Data Fig. 4 | Plasmid labeling of *E. faecalis* strains. CARD-FISH of *E. faecalis* DSM 8630 (as a negative control) and *E. faecalis* MM1 using the specific 1,3-PD probe. Scale bar is indicated.

High similarity of isolate genome to *E. faecalis*

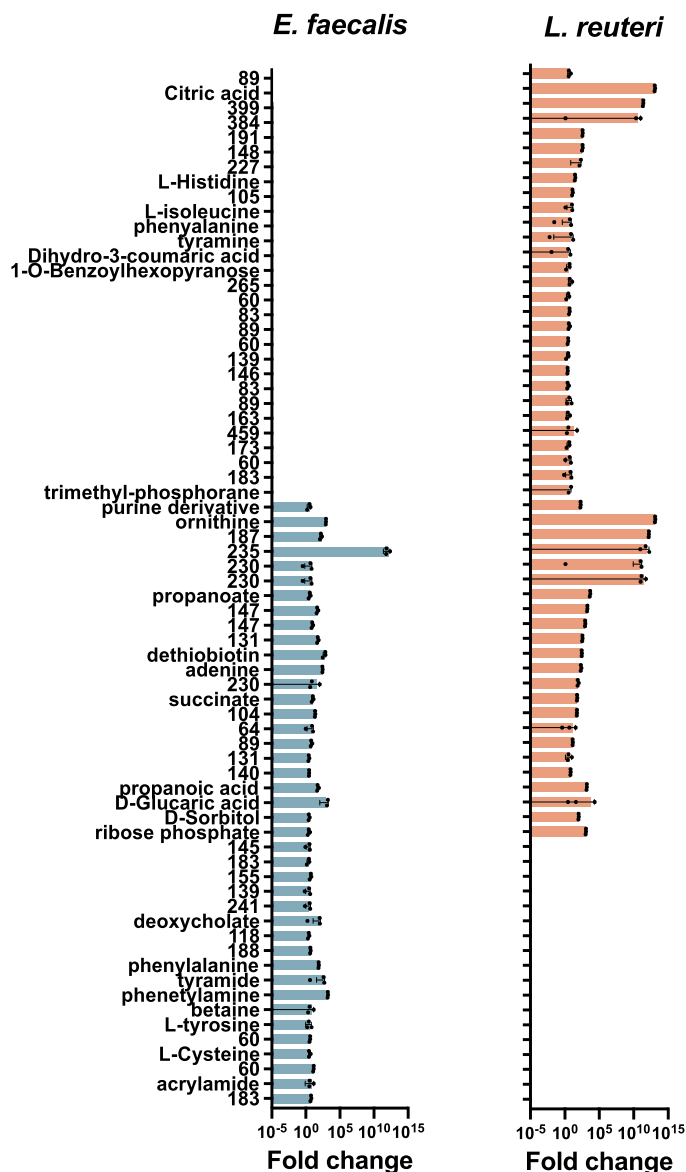


Extended Data Fig. 5 | Similarity of the *E. faecalis* strains MM1 and DSM 8630 genomes and predicted proteomes. Similarity of DNA contigs between the DSM 8630 and MM1 strains. Contigs were aligned using the Mauve genome alignment software⁶⁷.



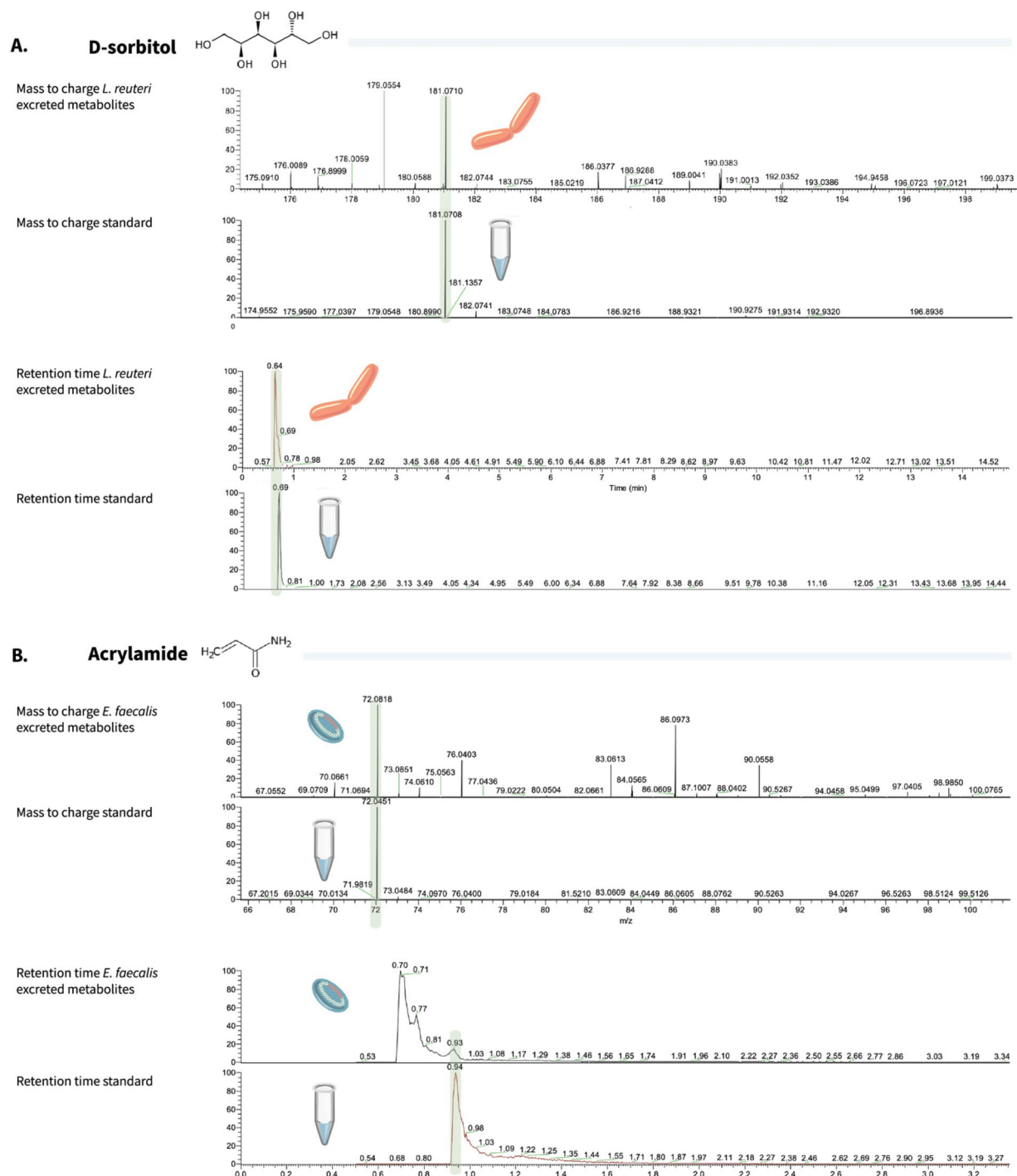
Extended Data Fig. 6 | Proximity assay between *L. reuteri* and *E. faecalis* strains. Left panel, the bar graph displays the rounded distance of *E. faecalis* colonies to *L. reuteri* colonies with reuterin in the media. Stars represent statistical significance with two-sided t-test of P value 0.017 (*) or 0.00027 (***) without adjustment for multiple comparisons. Right panel, the bar graph represents the rounded colonies diameter of *E. faecalis* and *L. reuteri* strains

with reuterin in the media. For both panels, the assays were performed in eight biological triplicates for which actual values and median, are presented. Stars represent statistical significance with two-sided t-test of p value <0.01 (**) and <0.05 (*) without adjustment for multiple comparisons (P values from left to right, 0.0075, 0.0031, 0.0089 and 0.04).

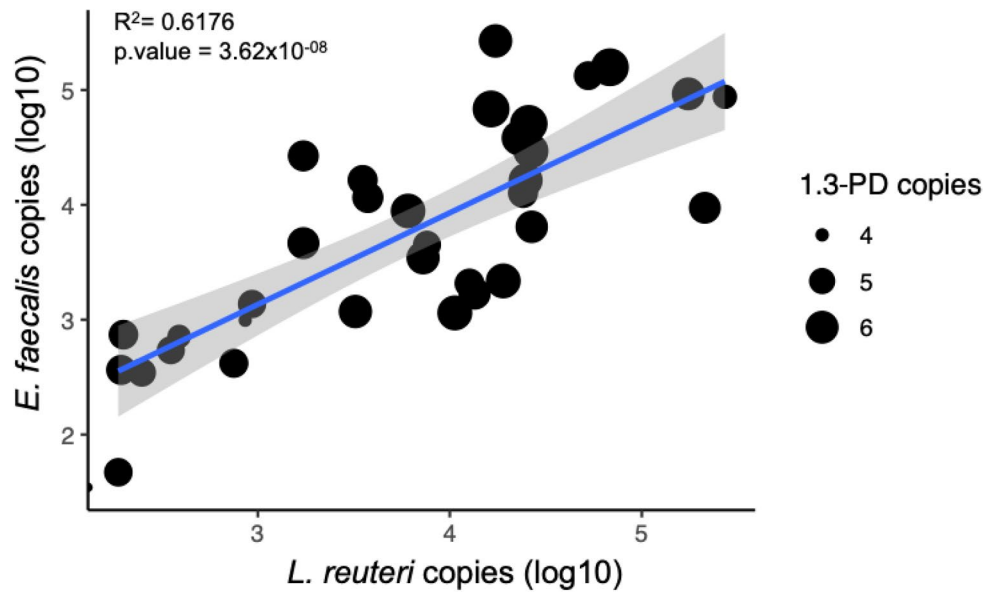


Extended Data Fig. 7 | Production of metabolites by *L. reuteri* and *E. faecalis*. LC-MS analysis of the metabolites produced by *L. reuteri* and *E. faecalis* cultured on basal medium (as compared to a blank medium) and spent medium of each other (as compared to the spent medium of the first inoculated strain), as represented by graphs displaying the fold change of the produced metabolites

(fold change for production defined as the ratio of [metabolites after growth/ metabolites before growth] equal or superior to 2.5). All LC-MS measurements were performed on biological triplicates for which actual values, mean, and standard deviations are presented. The y-axis gives the mass of the metabolites (m/z) or the annotations when available.



Extended Data Fig. 8 | Validation of exchange metabolites by LC-MS using commercially available standards. Mass-to-charge and retention time chromatograms are given for D-sorbitol (A) and acrylamide (B) in experimental samples and standard solutions.



Extended Data Fig. 9 | Linear regression model between *L. reuteri* and *E. faecalis* abundance in 34 rumen samples. The data was log₁₀ transformed before fitting the linear model with the lm function in R (version 4.2.1). The simple linear regression model statistical test was used, and the *P* value two-sided

with no correction for multiple comparisons. The shaded area in gray represents confidence intervals (95%). The circle sizes represent the 1,3-PD gene copies number.

Reporting Summary

Nature Portfolio wishes to improve the reproducibility of the work that we publish. This form provides structure for consistency and transparency in reporting. For further information on Nature Portfolio policies, see our [Editorial Policies](#) and the [Editorial Policy Checklist](#).

Statistics

For all statistical analyses, confirm that the following items are present in the figure legend, table legend, main text, or Methods section.

n/a | Confirmed

- The exact sample size (n) for each experimental group/condition, given as a discrete number and unit of measurement
- A statement on whether measurements were taken from distinct samples or whether the same sample was measured repeatedly
- The statistical test(s) used AND whether they are one- or two-sided
Only common tests should be described solely by name; describe more complex techniques in the Methods section.
- A description of all covariates tested
- A description of any assumptions or corrections, such as tests of normality and adjustment for multiple comparisons
- A full description of the statistical parameters including central tendency (e.g. means) or other basic estimates (e.g. regression coefficient) AND variation (e.g. standard deviation) or associated estimates of uncertainty (e.g. confidence intervals)
- For null hypothesis testing, the test statistic (e.g. F , t , r) with confidence intervals, effect sizes, degrees of freedom and P value noted
Give P values as exact values whenever suitable.
- For Bayesian analysis, information on the choice of priors and Markov chain Monte Carlo settings
- For hierarchical and complex designs, identification of the appropriate level for tests and full reporting of outcomes
- Estimates of effect sizes (e.g. Cohen's d , Pearson's r), indicating how they were calculated

Our web collection on [statistics for biologists](#) contains articles on many of the points above.

Software and code

Policy information about [availability of computer code](#)

Data collection

no software was used

Data analysis

The plasmidomes of 78 Holstein dairy cows were retrieved from the raw reads of sequenced metagenomes, using the Recycler algorithm. Plasmid-containing 1,3-PD genes were retrieved using local Blast. The plasmid was analysed for the presence of conjugative systems and relaxases using ConJScan of McSyFinder and MOBscan. The raw reads of 311 healthy human individual fecal samples from project SRP100518 were trimmed using Trim Galore, assembled into contigs by Megahit and plasmids were recovered by SCAPP. Raw reads of each of the 311 samples were mapped to plasmid sequence of interest using BBmap, and the plasmid was considered present in a sample if its read coverage was higher than 70% as computed by SAMtools mpileup. MassLynx and TargetLynx software (v.4.2, Waters) were applied for the acquisition and analysis of data of targeted metabolomics of reuterin compound. ESV table was created using DADA2 and QIIME. The sequences from shotgun sequencing were assembled with SPAdes. The DNA contents of the bacterial strains were compared using Mauve, and Proteinortho. For STORM microscopy, image acquisition and data reconstruction were performed using the Elyra PS1 system (X100 oil objective) and Zen software (Zeiss). Quantitative PCR standard curves were obtained using eight dilution points and were calculated using the Rotorgene 6000 series software (Qiagen, Hilden, Germany). For untargeted metabolomics, chromatogram processing, peak detection and integration was performed using MZmine 2 with signal to noise ratio set to 5 (MZmine-2.41.2). Metabolite annotations were obtained by performing Molecular Networking using the GNPS, by using the Compound Discoverer version 3.3 (Thermo Scientific), by extracting the metabolites present in the KEGG genomes of the bacteria and using MetaboAnalyst.

For manuscripts utilizing custom algorithms or software that are central to the research but not yet described in published literature, software must be made available to editors and reviewers. We strongly encourage code deposition in a community repository (e.g. GitHub). See the Nature Portfolio [guidelines for submitting code & software](#) for further information.

Data

Policy information about [availability of data](#)

All manuscripts must include a [data availability statement](#). This statement should provide the following information, where applicable:

- Accession codes, unique identifiers, or web links for publicly available datasets
- A description of any restrictions on data availability
- For clinical datasets or third party data, please ensure that the statement adheres to our [policy](#)

Genomes sequencing of *E. faecalis* MM1 and DSM 8630 have been deposited in GenBank (JAMKBU000000000 and JAMKBV000000000). Metabolomics data was deposited to MetaboLights under the identifier MTBLS7248 (www.ebi.ac.uk/metabolights/MTBLS7248).

Research involving human participants, their data, or biological material

Policy information about studies with [human participants or human data](#). See also policy information about [sex, gender \(identity/presentation\), and sexual orientation](#) and [race, ethnicity and racism](#).

Reporting on sex and gender

Reporting on race, ethnicity, or other socially relevant groupings

Population characteristics

Recruitment

Ethics oversight

Note that full information on the approval of the study protocol must also be provided in the manuscript.

Field-specific reporting

Please select the one below that is the best fit for your research. If you are not sure, read the appropriate sections before making your selection.

Life sciences Behavioural & social sciences Ecological, evolutionary & environmental sciences

For a reference copy of the document with all sections, see nature.com/documents/nr-reporting-summary-flat.pdf

Life sciences study design

All studies must disclose on these points even when the disclosure is negative.

Sample size

all experiments were performed with at least biological triplicates when the biological signal was the most reproducible and up to ten biological replicates in experiments where high deviations were expected

Data exclusions	no data was excluded
Replication	Each experiment was repeated 3 times in triplicates (or more). All attempts in replication were successful.
Randomization	in our experiments we measure the effect of one parameter to another (i.e. enzymatic activity of an enzyme to its substrate ..), thus no randomization was considered
Blinding	no blinding was considered as most of the experiments were performed by one person

Reporting for specific materials, systems and methods

We require information from authors about some types of materials, experimental systems and methods used in many studies. Here, indicate whether each material, system or method listed is relevant to your study. If you are not sure if a list item applies to your research, read the appropriate section before selecting a response.

Materials & experimental systems

n/a	Included in the study
<input checked="" type="checkbox"/>	<input type="checkbox"/> Antibodies
<input checked="" type="checkbox"/>	<input type="checkbox"/> Eukaryotic cell lines
<input checked="" type="checkbox"/>	<input type="checkbox"/> Palaeontology and archaeology
<input checked="" type="checkbox"/>	<input type="checkbox"/> Animals and other organisms
<input checked="" type="checkbox"/>	<input type="checkbox"/> Clinical data
<input checked="" type="checkbox"/>	<input type="checkbox"/> Dual use research of concern
<input checked="" type="checkbox"/>	<input type="checkbox"/> Plants

Methods

n/a	Included in the study
<input checked="" type="checkbox"/>	<input type="checkbox"/> ChIP-seq
<input checked="" type="checkbox"/>	<input type="checkbox"/> Flow cytometry
<input checked="" type="checkbox"/>	<input type="checkbox"/> MRI-based neuroimaging